ALTERNATIVE FUELS AND CHEMICALS FROM SYNTHESIS GAS

DOE/PC/93052--T2

Quarterly Status Report No. 2

For the Period 1 January - 31 March 1995

Contractor

AIR PRODUCTS AND CHEMICALS, INC.
7201 Hamilton Boulevard
Allentown, PA 18195-1501

Prepared for the United States Department of Energy
Under Contract No. FC22-95PC93052
Contract Period 29 December 1994 - 28 December 1997

ALTERNATIVE FUELS AND CHEMICALS FROM SYNTHESIS GAS

Quarterly Status Report No. 2

For the Period 1 January - 31 March 1995

Contractor

AIR PRODUCTS AND CHEMICALS, INC.
7201 Hamilton Boulevard
Allentown, PA 18195-1501

Prepared for the United States Department of Energy
Under Contract No. FC22-95PC93052
Contract Period 29 December 1994 - 28 December 1997

DISCLAIMER

Alternative Fuels and Chemicals from Synthesis Gas

Quarterly Technical Progress Report

1 January - 31 March 1995

Contract Objectives

The overall objectives of this program are to investigate potential technologies for the conversion of synthesis gas to oxygenated and hydrocarbon fuels and industrial chemicals, and to demonstrate the most promising technologies at DOE's LaPorte, Texas, Slurry Phase Alternative Fuels Development Unit (AFDU). The program will involve a continuation of the work performed under the Alternative Fuels from Coal-Derived Synthesis Gas Program and will draw upon information and technologies generated in parallel current and future DOE-funded contracts.

Summary of Activity

- Several meetings were held between Process, Operations, and R&D to come up with a run plan for the hydrodynamic/methanol run scheduled in June 1995. Some changes were made in previously agreed objectives. It was decided not to start up the old reactor (F-T) system. Modifications and associated expenditure needed to operate the F-T train for methanol synthesis are significant. In view of the current budgetary constraints, it was decided to defer the "cleanup" and hydrodynamic study in the F-T reactor until the next F-T campaign. In order to take advantage of availability of the new reactor (methanol) system, an additional objective to evaluate an alternate methanol catalyst was added to the new reactor run plan. This objective was originally deferred until 1996. Certainly, it is more cost-effective to address several objectives in one reactor system than to study fewer objectives in two systems. Centrifugal testing of the spent slurry to separate spent catalyst and oil was dropped as it appears that this method is not commercially viable because of high capital costs. The run will last nominally 3 weeks, with a 1-week operation on BASF S3-86 catalyst and a 2-week operation on Haldor-Topsoe MK-101 catalyst. A table of the current run plan is attached. The target start-up date is June 1.

  CO reduced BASF S3-86 methanol catalyst showed about the same level of initial activity and subsequent deactivation in the laboratory compared to using H_2 as the reduction gas.

  A preliminary hazards review was conducted on March 2 for the modifications needed for this run. Facility Change Notice (FCN) forms will be filled out and reviewed next month.

- Radian Corporation completed its evaluation of the air permit issues for the next LaPorte run scheduled for June 1995. After discussions with TNRCC personnel, Radian proposed several options. Air Products has decided to follow the alternative to the exemption option by reverting the old reactor configuration to the one originally permitted by TNRCC. By physically disconnecting the high pressure reactor feed system, we will eliminate the

possibility of increasing production or emission rates. We will not remove the new internal heat exchanger, as the heat exchanger alone does not increase production or emissions rates. As suggested by Radian, we will internally document this and other modifications for Air Products' files.

- In DME studies, work has focused on use of the new Robinson-Mahoney reactor. Since the Robinson-Mahoney (RM) internals immobilize the catalyst, it is valuable to develop samples for further analysis; however, this immobility also causes a mass transfer limit which makes interpretation of the life studies difficult unless a long run is carried out. The last life run using the RM internals was carried out long enough to show that deactivation of the catalyst system was significantly reduced by the immobilization of the catalyst particles. Subsequent testing of the catalyst particles from the RM experiment showed that the dehydration catalyst had been deactivated, but to a lesser extent than if the reaction had been carried out in a standard slurry reactor. The methanol catalyst had not deactivated. Thus we conclude that the intimate contact between particles is necessary for the level of deactivation experienced in the slurry reactor. This surprising result will be followed up and exploited in the next few months.

- A follow-up thorough analysis of the data from all dehydration catalyst screening runs, along with the results from the LPDME run using Robinson-Mahoney basket internals and pelletized catalysts, shows that the deactivation of both methanol and dehydration catalysts is not correlated with the activity of dehydration catalysts, at least for the long-term deactivation. *If one could reduce the intimate physical interaction* (e.g., collisions, intimate contact among fine powders) between the two catalysts, a stable catalyst system might be achievable.

- Following up on the lead provided by silica not affecting aging, a Condea silica alumina containing 15% alumina and 85% silica was tested as a MeOH dehydration catalyst. The catalyst system for DME using this material aged rapidly.

- In February four more dehydration catalysts were screened, including fumed alumina, zirconia, zirconia-modified silica gel, and WO_3-modified Catapal alumina. None exhibited better activity and stability than Catapal B alumina. We have been able to identify several distinct modes of deactivation, e.g., deactivation of both catalysts or deactivation of one component only. This understanding suggests new directions in the search for alternate dehydration catalysts.

- Three more dehydration catalysts were screened in March, including a silica alumina containing 95% of SiO_2, a calcium phosphate catalyst (hydroxyapatite), and a silica sample doped with phosphoric acid. None exhibited attractive performance.

- The University of Aachen reports that they have been able to reproduce the isobutanol productivity of Falter's best catalyst. Methanol formation rate is higher than the original catalyst. Unfortunately, this increased productivity is accompanied by a high rate of formation of unwanted methane.

- At Lehigh, the Cs-doped $Cu/ZnO/Cr_2O_3$) catalyst has been tested at 325°C for HAS under two reaction pressures (7.6 and 6.5 MPa) and five contact times with a syngas of H_2/CO of 0.75. At longer contact times (low space velocities), HAS seems to be enhanced by the lower reaction pressure. In addition the lower pressure decreases methanol formation.

- Professor Foley reports continued work on testing of alkali-doped catalysts precipitated with KOH. Temperatures necessary for isobutanol formation are still higher than desired for slurry operation, but progress over the initial set of catalysts is apparent.

- In early January, a literature search was conducted on heterogeneous carbonylation catalysts, and based on this a plan was generated for our goal of converting DME to EDA using a heterogeneous catalyst. The plan calls for the preparation of several rhodium catalysts. In particular, we will prepare $[Rh(diphos_2)]^+$ complexes and support them on different types of alumina, prepare supported Rh complexes on Reillex polymers, and also prepare a supported $Li[Rh(CO)_2X_2]$. We will also attempt to intercalate an anionic Rh complex within the layers of a double hydroxide.

- During February, a first attempt was made to prepare a heterogeneous rhodium catalyst for the conversion of dimethyl ether to ethylidene diacetate (EDA). A sample of Reillex 425 polymer was loaded with a solution of $Rh_2(CO)_4Cl_2$ in toluene (2% by weight Rh). During March, we tested this material as a heterogeneous catalyst for the conversion of dimethyl ether (DME) to ethylidene diacetate (EDA). The catalytic performance of the heterogeneous catalyst was compared with the analogous homogeneous system using similar experimental conditions (syngas, 190°C, 1500 psi). In the absence of lithium iodide, the heterogeneous catalyst worked much better than the homogeneous analog forming acetic anhydride, acetaldehyde and EDA. Adding lithium iodide did not improve the performance of the heterogeneous system, but it did help the homogeneous system produce EDA, although the productivity was still less than that of the heterogeneous system.

- Various previously tested catalysts for isobutanol synthesis from methanol (Ag/K on SrO and Ag/Cs on SrO) were retested to determine reactor reproducibility. In addition, the best catalyst was prepared again, tested, and identical results were obtained. By varying the mol ratio of Ag/Cs on SrO, it was determined that an Ag/Cs mol ratio of 1 favors higher selectivity to oxygenates. This suggests Ag/Cs ratios of less than 1 should be screened. An IR of used Ag/Cs on SrO catalyst shows carbonate bands. However, Ag on $SrCO_3$ is inactive as a catalyst.

- Final details were made to the subcontract with Bechtel. This subcontract was officially in place at the end of March. Bechtel's first priority is in defining isobutanol catalyst performance targets to achieve a final MTBE product at 70¢/gal.

RESULTS AND DISCUSSION

TASK 1: ENGINEERING AND MODIFICATIONS

1.1 Liquid Phase Hydrodynamic Run

Radian Corporation completed its evaluation of the air permit issues for the hydrodynamic/methanol run scheduled for June 1995. No permit/exemption action is needed for the new reactor as its operation is covered by the 1994 exemption. The key question for the old reactor was whether disconnecting an additional feed source (high pressure hydrogen) to limit methanol production would be acceptable to TNRCC. Radian worked with TNRCC to resolve this issue. After discussions with TNRCC personnel, Radian proposed several options. While most options required an exemption application, Air Products decided to follow an alternative to the exemption options by reverting the old reactor configuration to the one originally permitted by TNRCC. By physically disconnecting the high pressure reactor feed system, the possibility of increasing production or emission rates will be eliminated. However, the new internal heat exchanger will not be removed, as the heat exchanger alone does not increase production or emission rates. As suggested by Radian, we will internally document these and other modifications for Air Products' files.

Several meetings were held between Process, Operations and R&D to come up with a run plan. Some changes were made in previously agreed-to objectives. It was decided not to start up the old reactor (F-T) system. Modifications and associated expenditure needed to operate the F-T train for methanol synthesis are significant. In view of the current budgetary constraints, it was decided to defer the "cleanup" and hydrodynamic study in the F-T reactor until the next F-T campaign. In order to take advantage of availability of the new reactor (methanol) system, an additional objective to evaluate an alternate methanol catalyst was added to the new reactor run plan. This objective was originally deferred until 1996. Certainly, it is more cost-effective to address several objectives in one reactor system than to study fewer objectives in two systems. Centrifuge testing of the spent slurry was dropped as it appears that this method is not commercially viable because of high capital costs. During the design of Tennessee Eastman's Kingsport LPMEOH™ plant, it was determined that incineration of spent slurry was more economical then separating catalyst and oil using a centrifuge. The run will last nominally three weeks, with a one-week operation on BASF S3-86 catalyst and a two-week operation on Haldor-Topsoe MK-101 catalyst. The current run plan is summarized in Table 1.1.1. The target start-up date is June 1.

A preliminary hazards review was conducted on March 2 for the modifications needed for this run. Facility Change Notice (FCN) forms will be filled out and reviewed in April. Catalyst orders were placed for LaPorte: 3000 lbs of BASF S3-86 catalyst (1 + 1 spare charge) and 1500 lbs of Haldor-Topsoe MK-101 catalyst (1 charge).

1.2 and **1.3** No progress to report this quarter.

Table 1.1.1. LaPorte AFDU LPMEOH/Hydrodynamics Run - June 1995

Run No.	No. of Days	Comment	Gas Type	Reactor Pressure psia	Reactor Temp. deg F	Space Vel. sL/kg-hr	React. Fd. lbmol/hr	Inlet Sup. Vel. ft/sec	Slurry wt% oxide	Lb Cat. oxide	Approx. MeOH Prodtn, GPD
NEW REACTOR (27.20) / BASF CATALYST											
	3	Carbonyl Burnout, Dephlegmator Testing	Texaco								
AF-A9	1	Kingsport Reduction	4% CO in N2	60		1500				1177	
AF-R13.1	2	Base Case	Texaco	765	482	7000	367.5	0.83	42	1177	3790
AF-R13.2	3		Kingsport	750	482	4000	210	0.47	40	1177	3320
AF-R13.3	2		Texaco	765	482	10000	525	1.2	43	1177	4850
Total	11										27240
NEW REACTOR (27.20) / HALDOR-TOPSOE CAT											
AF-A10	1	Kingsport Reduction	4% CO in N2	60		1500				1177	
AF-R14.1	2	Base Case	Texaco	765	482	7000	367.5	0.83	42	1177	3790
AF-R14.2	3		Kingsport	750	482	4000	210	0.48	40	1177	3320
AF-R14.3	1.5		Texaco	765	482	10000	525	1.2	43	1177	4850
AF-R14.4	1.5		Texaco	765	482	4000	210	0.47	41	1177	2340
AF-R14.5	1	Base Case	Texaco	765	482	7000	367.5	0.83	42	1177	3790
AF-R14.6	3	Tracer Study	Texaco	765	482	4000-10000	210-525	0.47-1.2	40-43	1177	3790
Total	13										43485
GRAND TOTAL	24										

1.4 AFDU R&D Support

1.4.1 Catalyst Activation With CO

One of the objectives of the methanol/hydrodynamics run in the AFDU at LaPorte will be to demonstrate new technology proposed for Kingsport. To simplify the process equipment and procedure for catalyst reduction in the Liquid Phase Methanol plant design for Eastman, a new reduction procedure for BASF S3-86 was investigated in the lab. The goal of the new reduction procedure was to eliminate H_2O production during reduction by using H_2-free reduction feed gas, decrease the time required for reduction, and simplify the temperature ramping procedure. To this end, reduction of S3-86 was carried out in the lab autoclave using CO in N_2 feed gas (H_2-free). The activity and life of the catalyst were also tested.

Background

The current design for the Liquid Phase Methanol plant at the Eastman Chemical Company complex includes a catalyst reduction vessel from which slurry containing fresh, reduced catalyst will be supplied to the process. The heretofore established reduction procedure for the BASF S3-86 catalyst involves an empirically established temperature ramping protocol and the use of H_2-containing reduction gases (either 2% H_2 in N_2 or 4% Texaco syngas in N_2). The use of H_2 as a reductant results in the production of H_2O via CuO reduction:

$$H_2 + CuO \rightarrow Cu + H_2O.$$

However, H_2O production during reduction complicates downstream processing since slurry mineral oil vaporized during reduction and H_2O may form two phases and the H_2O produced must be processed as waste water.

To investigate the possibility of simplifying the process equipment and operating procedure for catalyst reduction, a new reduction procedure was investigated in the 300 cc lab autoclave. The goal of the new reduction procedure is to minimize water production during reduction, decrease the time required for reduction, and simplify the temperature ramping procedure. In this experiment, a nominal 2% CO in N_2 reduction gas was used. Thus, CuO is reduced by CO:

$$CO + CuO \rightarrow Cu + CO_2,$$

which eliminates H_2O as a direct product of reduction.

Experimental

The time-temperature ramp was simplified. The previously established procedure involved a 12 hr temperature hold at 200°C during the overall increase from 100°C to 240°C. For the present experiment, the temperature was increased from 100°C to 240°C at 10°C/hr continuously, thereby saving 12 hr in the reduction procedure. A feed flow rate of 1500 std.lit./kg-hr and a pressure of 50 psig were chosen.

Reduction with 2% CO-98% N_2

Figure 1.4.1 shows the time temperature profile used for this experiment.

Figure 1.4.1. Temperature Ramp Used for Catalyst Reduction

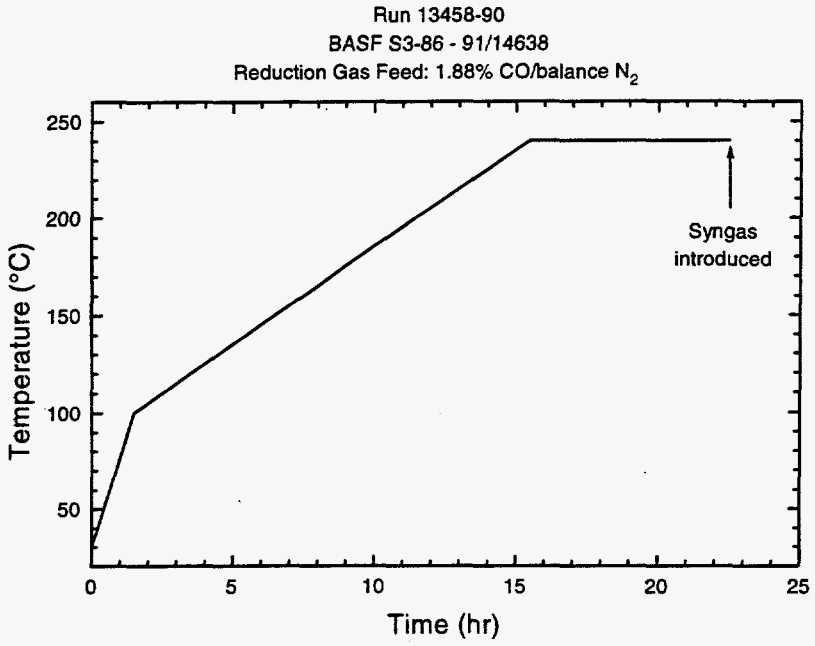

Syngas introduction was delayed for several hours after 240°C was reached so that the feed could be switched during normal working hours. As shown below, very little occurs during the 240°C hold. In practice, the feed could be switched as soon as the reactor temperature reaches 240°C.

The reactor effluent concentrations of CO, CO_2, H_2O, and H_2 during reduction were obtained by GC. The GC was calibrated for H_2O using a controlled temperature and pressure H_2O saturator. For low concentrations, a sub-0°C condenser (freezer) was used downstream of the H_2O saturator. Water concentration was calculated from the vapor pressure of liquid or solid H_2O at the saturator or freezer temperature. The GC response was slightly non-linear, necessitating the use of a calibration curve. Quantitation accuracy for H_2O was ±10% (relative) for H_2O concentrations greater than 0.1 mol%, but the detection limit was about 0.025 mol%.

Figure 1.4.2 shows the reactor effluent concentrations of CO, CO_2, H_2O, and H_2 during reduction plotted as a function of the reduction temperature.

Figure 1.4.2. Reactor Exit Concentration versus Reduction Temperature

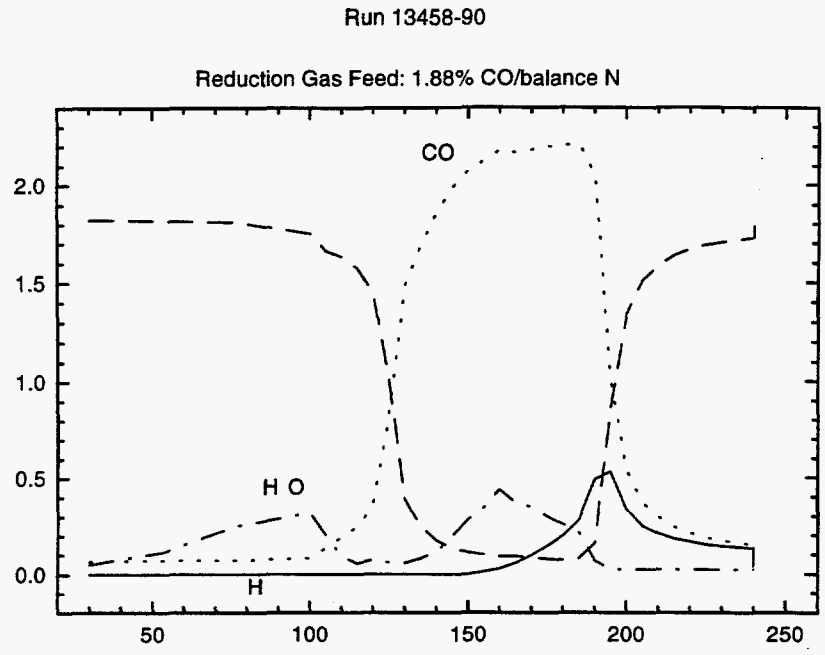

Clearly, CO is consumed, while CO_2, H_2O, and H_2 are produced during reduction.

Figure 1.4.3 shows the cumulative consumption of CO and the cumulative production of CO_2, H_2O, and H_2 versus reduction temperature.

Figure 1.4.3. Cumulative Consumption/Production versus Reduction Temperature

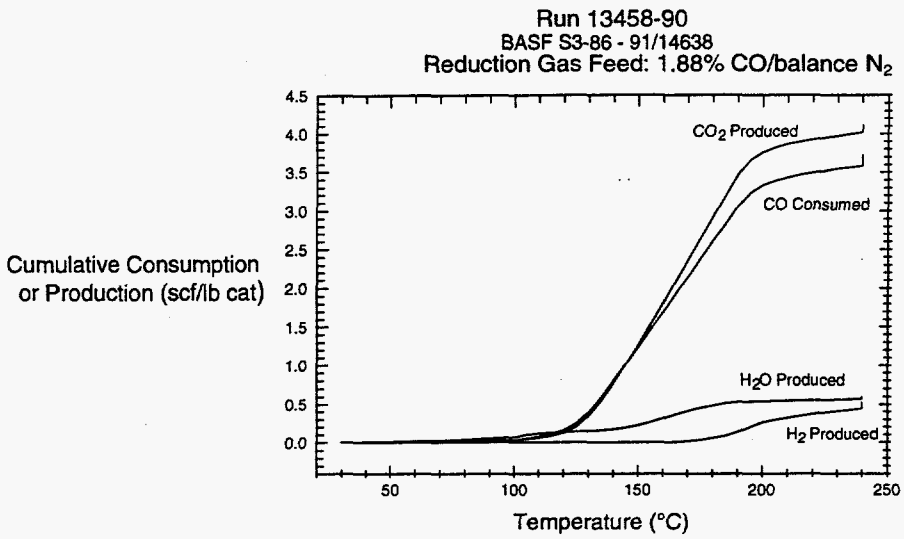

The use of the CO/N_2 feed gas did not completely eliminate H_2O production during reduction. Approximately 0.55 scf of H_2O/lb of as-received catalyst was produced during reduction. This detection of unexpected H_2O was examined in detail.

The presence of two peaks in the water concentration profile in Figure 1.4.2 suggests that H_2O is derived from two different sources during reduction. The low temperature peak probably corresponds to the loss of physically adsorbed H_2O that has been retained after calcination or adsorbed during handling after calcination. The second peak is probably produced from decomposition of the "hydroxy-carbonate" precursor that constitutes the as-received catalyst. This hydroxy-carbonate precursor eliminates hydroxide groups as H_2O during heat-up.

The H_2 produced in the later stage of reduction results from H_2O reacting with CO via the water-gas shift reaction:

$$CO + H_2O \leftrightarrow H_2 + CO_2.$$

Thermodynamic equilibrium for the exothermic shift reaction lies very far to the right for the temperature range of reduction, thereby representing a possible "sink" for H_2O during reduction. The equilibrium constant, Kp, ranges from 3600 at 100°C to 105 at 240°C. However, the data show that the shift reaction was far from equilibrium at any point during reduction up to 190°C. At temperatures greater than 190°C, the H_2O concentration was below the detection limit, so it was impossible to determine whether the shift reaction was close to equilibrium.

Comparison of the present results with results from a "standard" reduction using 4% syngas in N_2, for which a slower temperature ramp was also used, reveals corroborating evidence. Figure 1.4.4 shows the cumulative consumption of CO and H_2 (H_2 is first consumed and then produced during reduction with syngas) and the cumulative production of CO_2 and H_2O.

Figure 1.4.4. Cumulative Consumption/Production versus Temperature for Reduction Using 4% Syngas in N_2

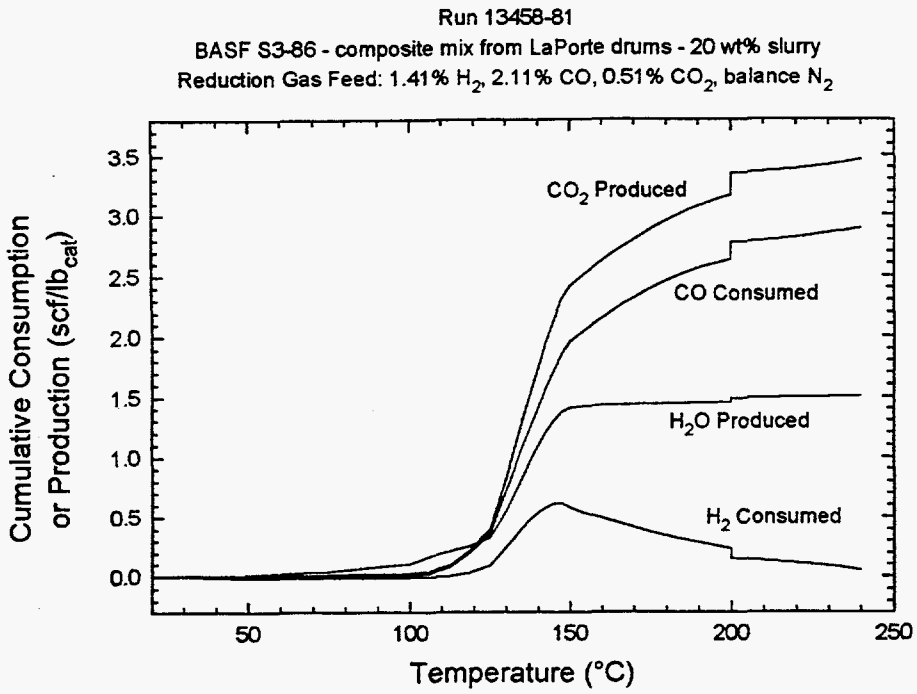

As expected, the H_2O produced for the H_2-containing reduction feed gas is higher: 1.5 scf of H_2O/lb versus 0.55 scf of H_2O/lb for the 2% CO/N_2 reduction gas. Again, the shift reaction is far from equilibrium for data points where the H_2O concentration was above the detection limit.

Activity of CO-Reduced (2% CO in N_2)

The catalyst activity after reduction using 2% CO/N_2 was measured at 250°C and 750 psig using Texaco syngas feed (35% H_2/51% CO/13% CO_2/1% N_2) at GHSVs of 5,000 and 10,000 std.lit./kg-hr. The expected performance and the results for the activity tests after reduction using 2% CO/N_2 are shown in Figure 1.4.5.

Figure 1.4.5. Performance of Catalyst After Reduction Using 2% CO in N_2

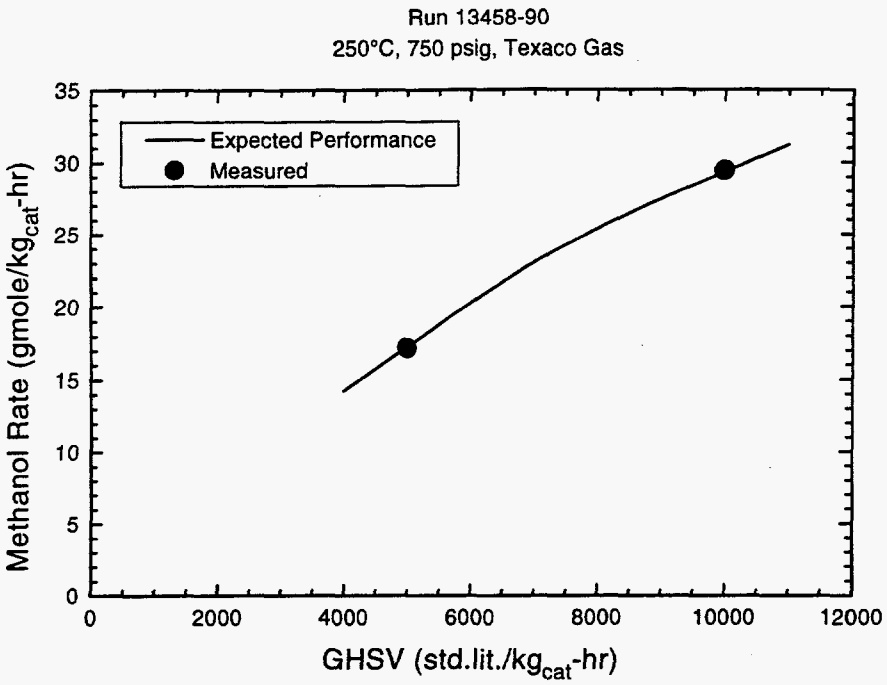

The expected performance curve was established by previous lab data for S3-86 after reduction in 4% syngas in N_2 or 2% H_2 in N_2 using slower temperature ramps. Clearly, reduction using 2% CO/N_2 and the faster temperature ramp produced a catalyst with the same performance as that obtained using the H_2-containing reduction gases.

Reduction and Performance Using 4% CO(Balance N_2)

H_2O production during reduction was not entirely eliminated but reduced by 63% compared to reduction by 4% syngas in N_2 (contains H_2). Even though the 2% CO reduction gas was H_2-free, H_2O was still produced from thermal desorption of physically adsorbed H_2O and dehydroxylation of the hydroxy-carbonate catalyst precursor. Also evident in this experiment was that the CO concentration was nearly zero during a portion of the temperature ramp, indicating almost complete consumption of the reductant.

In an attempt to avoid the complete consumption of reductant and to further reduce the production of H_2O during reduction, in situ reduction was done in the lab autoclave using a feed gas with a higher CO content (4% CO in N_2). The hypothesis was that the higher CO concentration may drive the water-gas shift reaction, $CO + H_2O = CO_2 + H_2$, to the right, thereby reducing H_2O production during reduction. Moreover, the use of higher CO concentration may avoid complete consumption of reductant, a situation that has an unknown, but possibly deleterious, effect on catalyst activation.

In situ reduction of S3-86 was carried out using the 300 cc autoclave system. The temperature ramp, pressure, and feed flow rate were the same as those used for the 2% CO in N_2 reduction experiment. Figure 1.4.6 compares the CO uptake and reactor exit CO concentration as a

function of temperature for reduction using 2% CO and 4% CO. The final consumption of CO is slightly higher for the 4% CO case, but probably not significantly different within the accuracy of the measurements. Also, the rate of CO consumption is faster for the 4% CO case, indicating a positive dependence of reduction rate on CO concentration. Note also that the lowest reactor exit CO concentration for the 4% CO feed case dropped to a minimum of 1 mol%, in contrast to the 2% CO feed case in which the reactor exit CO concentration fell nearly to zero.

Figure 1.4.6. The Effect of CO Feed Concentration on CO Consumption and Reactor Exit CO Concentration

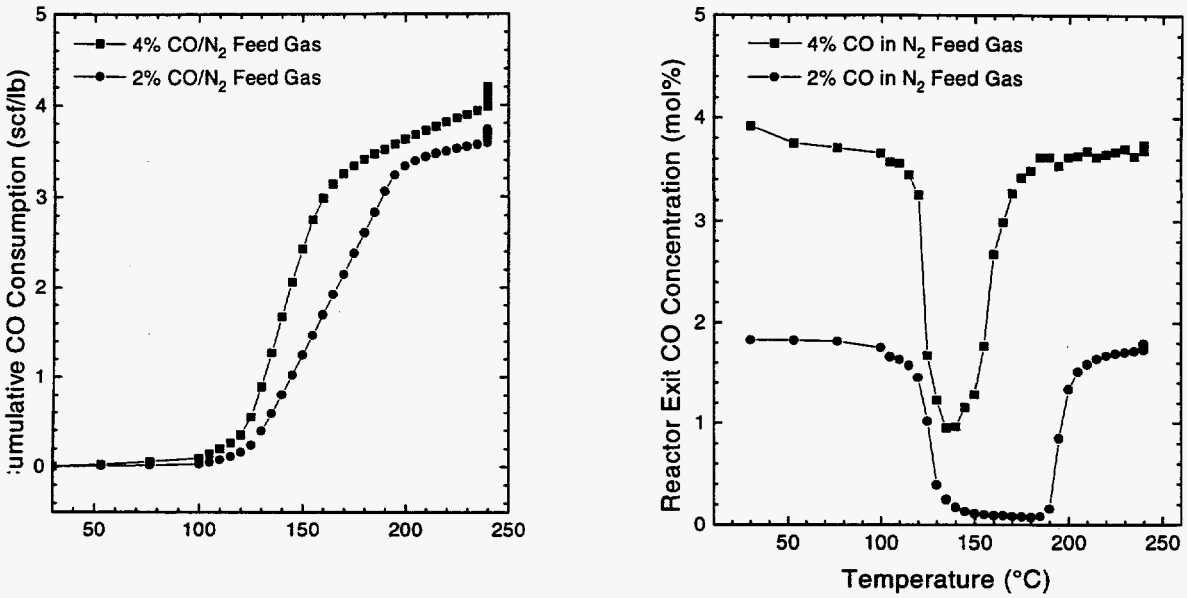

The fact that the CO concentration in the reactor was higher for 4% CO reduction apparently had no effect on the H_2O produced. The cumulative H_2O produced for the 4% CO reduction was estimated to be 0.65 scf/lb, which is comparable (within the experimental accuracy of the GC measurements) to the 0.55 scf/lb measured for the 2% CO reduction. Of course, these values are much lower than the 1.5 scf/lb measured for reduction using 4% Texaco gas in N_2. Evidently, the higher reactor CO concentration did not have a measurable effect on H_2O conversion via the water-gas shift reaction.

Reduction with 4% CO resulted in a catalyst with the same methanol synthesis activity as that obtained after reduction using the standard H_2-containing reduction gases. Figure 1.4.7 shows the measured performance after reduction with 4% CO and the expected performance curve after reduction using previously established reduction procedures and H_2-containing reduction gases. Clearly, the performance of the catalyst after the new reduction procedure equals that obtained for the previously established reduction procedure. Thus, in situ reduction of S3-86 with 4% CO in N_2 is a viable way of activating the catalyst.

Figure 1.4.7 Methanol Synthesis Rate after 4% CO Reduction
250°C, 750 psig, Texaco Gas

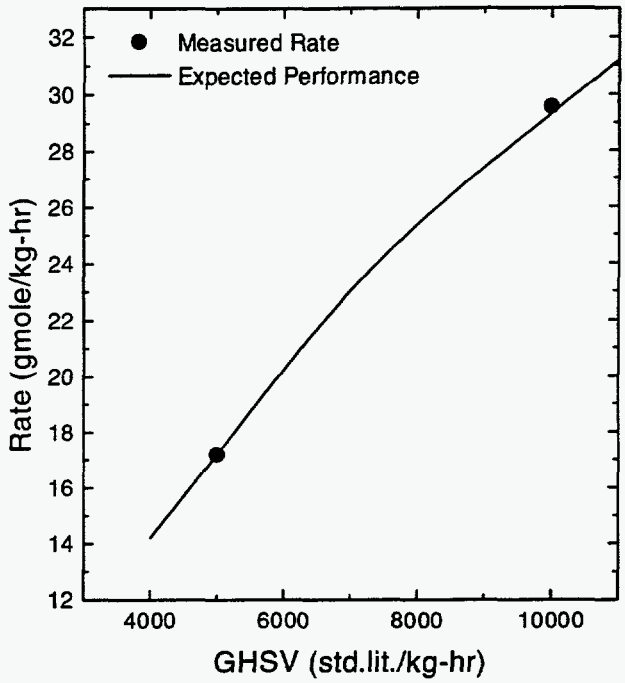

A new procedure that was changed slightly from the initial procedure to conserve CO was implemented. The data for the run are summarized in Figures 1.4.8-1.4.11. The heating rate and gas flow rate have been slightly modified from the initial run (Run 8--Figure 1.4.8). Gas uptake rate and product generation (Figs. 1.4.9-11) were satisfactory for all runs. The new procedure is substantially similar to the old procedure.

Figure 1.4.8 Reduction Temperature Profiles
4% Co/Balance N_2;
SV: 1,500 sl/kg-hr for 14191-50, 1,600 for 14045-08

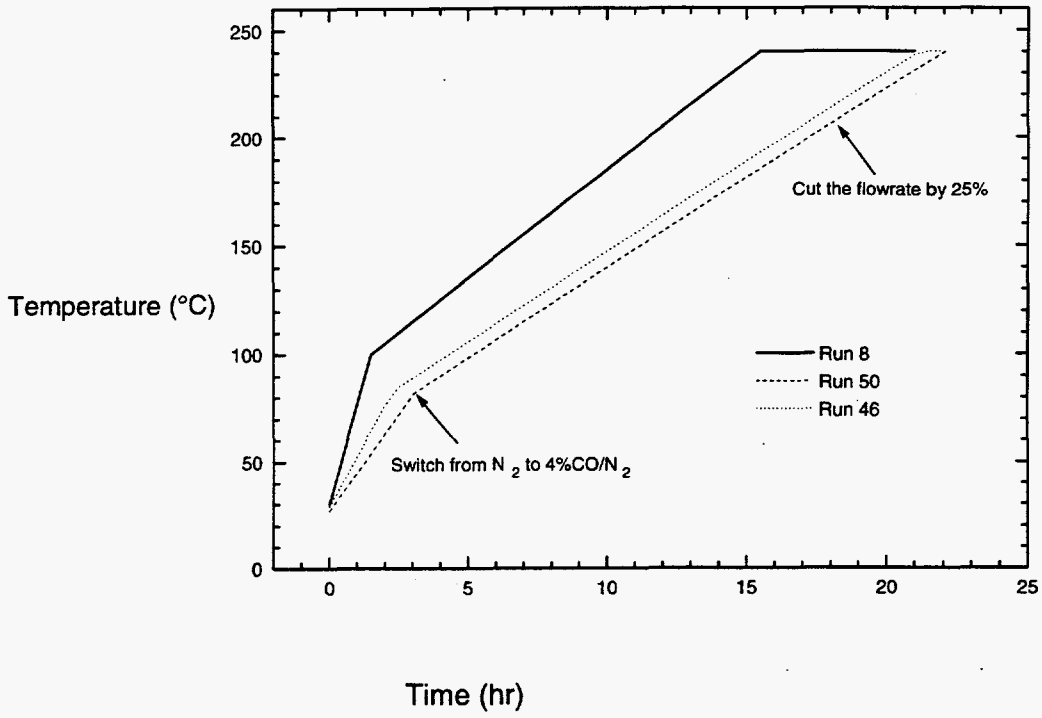

Figure 1.4.9 Runs 14191-50 and 14045-08
Reduction Gas Feed: 4% Co/Balance N_2;

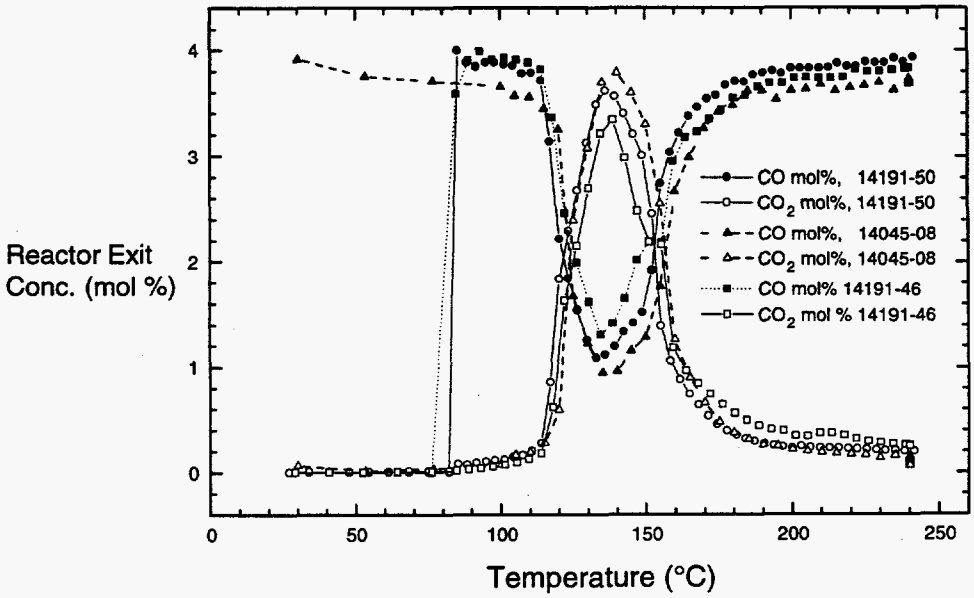

Figure 1.4.10 Runs 14191-50, 14191-46, anbd 14045-08
Reduction Gas Feed: 4% Co/Balance N_2

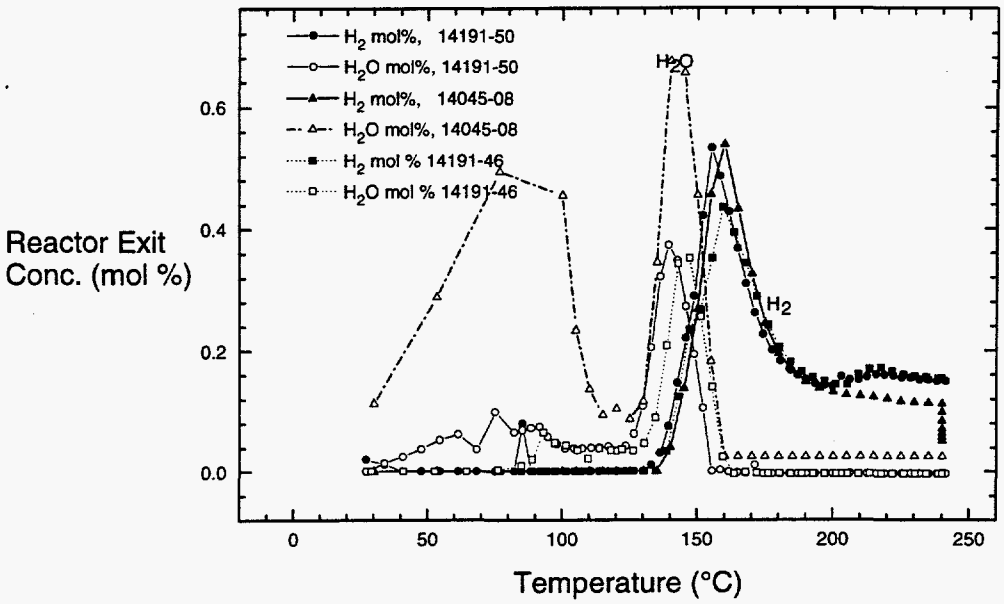

Figure 1.4.11 Comparison of Different Procedures
Runs 14191-50 and 14045-8 14191-46
BASF S3-886 - 91/14638

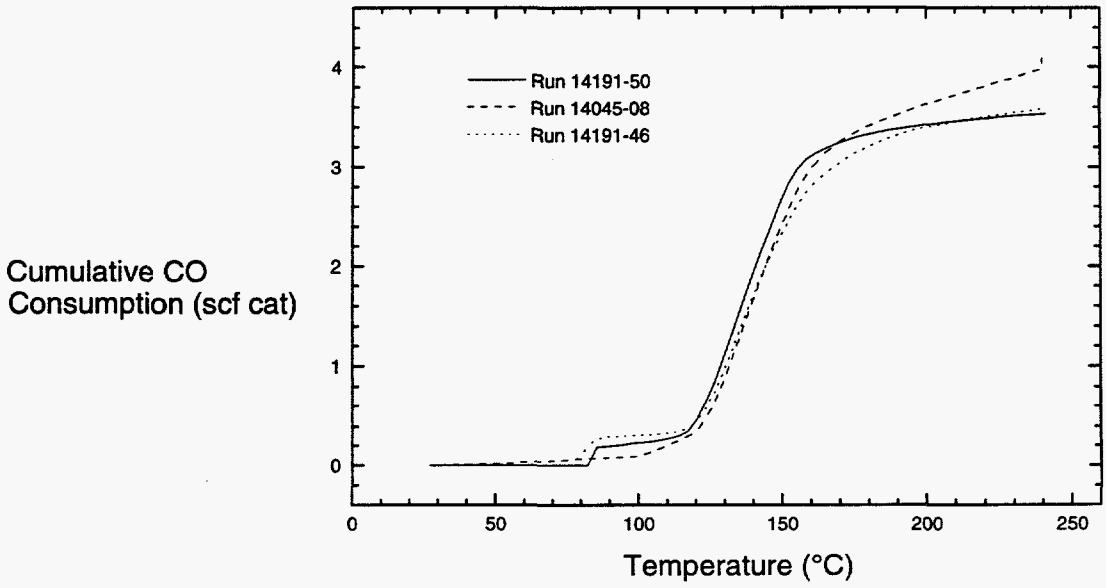

Life Test of Catalyst Activated Using CO

The final check on the CO activation procedure was to test the life of a CO-activated catalyst. Test results were analyzed by noting the change in specific rate constant with time. A decrease in rate constant translates to catalyst aging. To account for small differences in initial activity, aging is expressed as a % of the initial activity/unit time.

While the best kinetic expression available for methanol formation is not perfect, the correlation is good enough so that aging data can be compared. Since a CSTR is used for the rate measurement, the reaction conditions depend upon the activity of the catalyst. Using the rate expression allows comparison with experiments done at other conditions and accounts for small changes in operating conditions and catalyst activity.

Figure 1.4.12 shows historical data of activation with H_2 taken for the S3-86 catalyst. The slope of the line is a direct measurement of aging. The laboratory tests always show a higher aging rate than measured in the LaPorte test. The reasons for this difference are not clear. The laboratory test gives a fairly constant value for aging and thus, may be used as an indication of the relative stability of the catalysts.

Figure 1.4.12. S3-86 Deactivation in #1 300 cc Autoclave

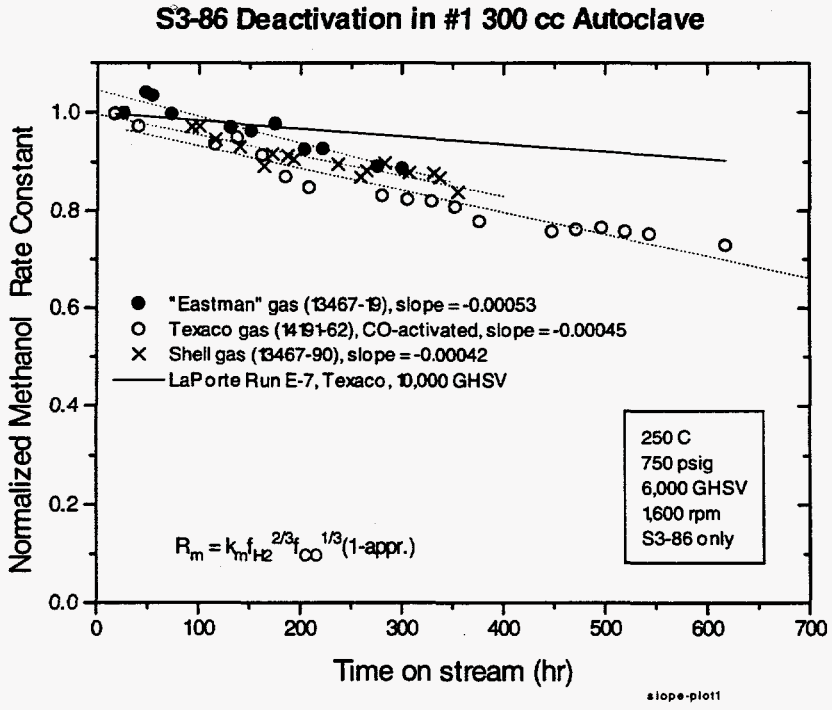

The data for CO activated catalyst are shown in Figure 1.4.13. The slope of the line from the laboratory data is about the same as for the laboratory data using the standard activation method. Therefore, we conclude that CO activation does not adversely affect the performance of the catalyst.

Figure 1.4.13. CO Reduction Comparison

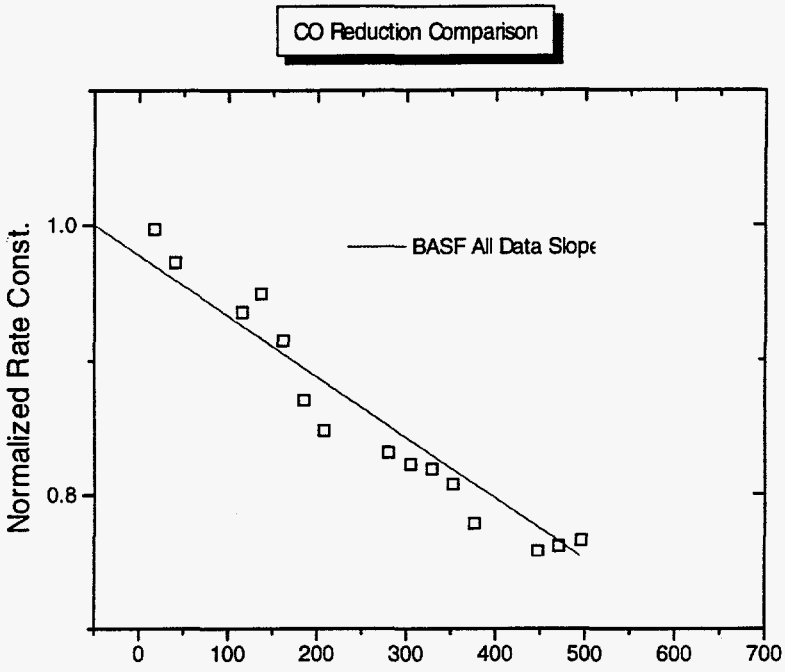

TASK 2: AFDU SHAKEDOWN AND OPERATIONS

2.1 Liquid Phase Hydrodynamic Run'

Nothing operationally to report this quarter. See Task 1.4 for run preparations.

TASK 3: RESEARCH AND DEVELOPMENT

3.1 New Processes for DME

The work this quarter focused on particular aspects of LPDME activity maintenance.

Dehydration Catalyst Screening Runs

In the previous quarterly we reported that an interaction between BASF S3-86 methanol catalyst and Catapal B γ-alumina is the cause of catalyst deactivation under LPDME conditions. This finding resulted in our active screening for alternative dehydration catalysts. In this quarter, nine more dehydration catalysts were examined, including two silica alumina, two modified Catapal B γ-alumina, a fumed alumina, two metal phosphate, and two ZrO_2-based samples. However, none exhibited better performance than γ-alumina.

Silica Alumina

Silica based materials are the preferred dehydration catalysts, since a previous experiment (14045-31) showed that a high surface area silica gel, while inert toward methanol dehydration, did not cause premature aging of the BASF S3-86 methanol catalyst. Two silica-aluminas of high silica content, i.e., Siral 85 (85% silica and 15% alumina) and Siral 95 from Condea, were

tested. The results for these two samples are shown in Table 3.1.1 and Figure 3.1.1 below, along with the results from a run using our standard catalyst system (S3-86 plus Catapal B γ-alumina). The methanol equivalent productivity of the systems containing Siral 85 and 95 is very low, e.g., at 20 hours onstream, 12.9 and 15.0 mol/kg-hr, respectively, compared to 30.7 mol/kg-hr for the standard catalyst system. This is due to both an extremely low dehydration activity and low methanol synthesis activity. The rate constants in Table 3.1.1 quantitate this observation. The results from these two experiments indicate that silica alumina is not a better dehydration catalyst than γ-alumina for our application.

Table 3.1.1. Kinetic Results from the Runs using S3-86 along with Siral 85 (14191-43), Siral 95 (13465-100), and Catapal B γ-alumina (11782-3), respectively

Run	Catalyst S3-86:Al2O3	Time on Stream (hr)	Productivity (mol/kg-hr) MEOH	DME	Equiv.	Rate Constant k_m[a]	k_d[b]
14191-43	80:20	20	8.5	2.2	12.9	1.0	1.2
13465-100	80:20	20	13.3	0.9	15.0	1.8	0.4
11782-3	82:18	20	2.1	14.3	30.7	2.6	17.0

a: Methanol synthesis rate constant calculated from $R_m = k_m f_{H_2}^{2/3} f_{CO}^{1/3} (1 - appr.)$, based on methanol catalyst weight.

b: Methanol dehydration rate constant calculated from $R_d = k_d f_{CO_2}^{-0.33} f_{MEOH}^{0.11} f_{CO}^{0.70} (1 - appr.)$, based on dehydration catalyst weight.

Figure 3.1.1 Catalyst screening using Siral 85 and Siral 95 plus S3-86

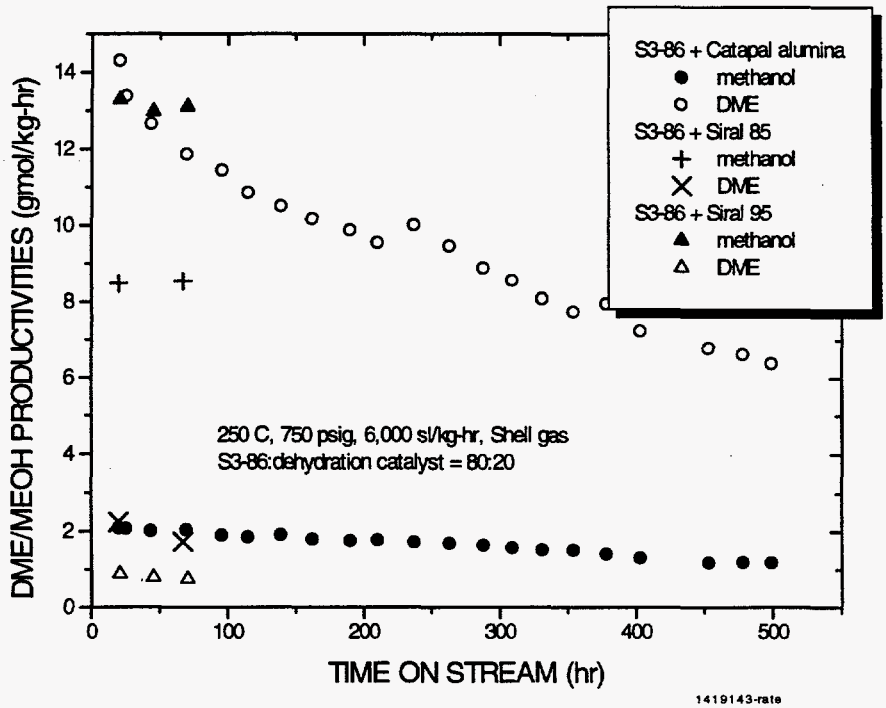

Two important observations should be noted, especially since they appear frequently in the series screening runs: First, different dehydration catalysts have different impacts on the methanol catalyst. The lower initial activity of the methanol catalyst in the catalyst systems containing silica alumina (see Table 3.1.1) indicates faster deactivation of the methanol catalyst in the presence of silica alumina than in the presence of γ-alumina. It is likely that this deactivation started during catalyst reduction. This occurs during the activation procedure for the methanol catalyst which runs 24 hr from room temperature to 240°C under diluted hydrogen before syngas is introduced into the system.

Second, different dehydration catalysts deactivate differently. The low dehydration activity from the silica alumina samples was unexpected, since silica alumina is normally more acidic than γ-alumina, and therefore should be more active toward dehydration. This low activity is attributed to the fast deactivation of silica alumina based on the following observation. We monitored the exit gas flow rate in the early hours of the run using Siral 85. Since the synthesis reaction is molecule-reducing, lower flow rate means greater activity. Judging by the flow rate shown in Table 3.1.2, the activity of the Siral 85 system at 1.2 hr on stream is fairly high, i.e., corresponding to a methanol equivalent productivity near 30 mol/kg-hr. Thus, we infer that the silica alumina had an initial dehydration activity at least comparable to the γ-alumina. However, this activity dropped considerably in the first 20 hr on stream as can be seen from the increasing flow rate. Again, it is likely that the activity of the silica alumina already started to drop during the reduction.

Table 3.1.2. Exit Gas Flow Rate as a Function of Time On Stream for the Run using Siral 85

Time on stream (hr)	Normalized exit flow rate[a]
1.2	0.79
4.3	0.85
20	0.89

a: Normalized by the inlet flowrate. For the run using S3-86 and Catapal γ-alumina, the normalized exit flowrate at 20 hr on stream is 0.77, corresponding to a methanol equivalent productivity of 30.7 mol/kg-hr.

Modified Catapal B γ-Alumina

One of our hypotheses about the interaction between the methanol and dehydration catalysts is that ZnO from the methanol catalyst might migrate onto alumina under the reaction conditions. The effect of this migration could be twofold: ZnO may deactivate the dehydration catalyst by reacting with the acid sites, and/or the methanol catalyst may lose its activity by losing its active component. If this is true, one would expect that:

1) the activity of the alumina would drop considerably if it is doped with ZnO; and
2) the doped Catapal B would result in a better stability of the methanol catalyst due to the smaller driving force for the migration.

Based on these considerations, a ZnO-doped Catapal B sample (14191-65) was prepared by impregnating the alumina with zinc nitrate, followed by calcination at 560°C for 4 hr to convert $Zn(NO_3)_2$ into ZnO and disperse ZnO on the alumina surface. The loading of ZnO is 40 wt%. According to the literature [Xie, et al., in: Adv. Catal., V37 (1990) p1], this corresponds to the highest loading of ZnO on alumina in atomically dispersed form. Further loading will result in ZnO crystallite formation.

Figures 3.1.2 and 3.1.3 display the activity of the catalyst system consisting of BASF S3-86 methanol catalyst and ZnO-Catapal B in comparison with that of the standard catalyst system (S3-86 plus virgin Catapal B). The reaction was run at the standard conditions (250°C, 750 psig, 6,000 GHSV, methanol:dehydration catalyst =80:20) using Shell gas. As expected, the ZnO-doped Catapal B has a lower dehydration activity than the virgin Catapal B. However, it shows little improvement in the stability of the methanol catalyst.

A WO_3-modified Catapal B γ-alumina was prepared by impregnating Catapal B γ-alumina with an aqueous solution of ammonium meta tungstate, followed by calcination at 700°C. Tungsten oxide has been reported in the literature to have dehydration activity at least as high as γ-alumina. This sample was tested along with BASF S3-86 methanol catalyst under the standard conditions using Shell gas (13465-58). Figures 3.1.2 and 3.1.3 show that the catalyst system does not exhibit better activity or stability than the standard catalyst system (S3-86 plus virgin Catapal B γ-alumina).

Figure 3.1.2. Methanol Synthesis Rate Constant as a Function of Time On Stream for Different Catalyst Systems

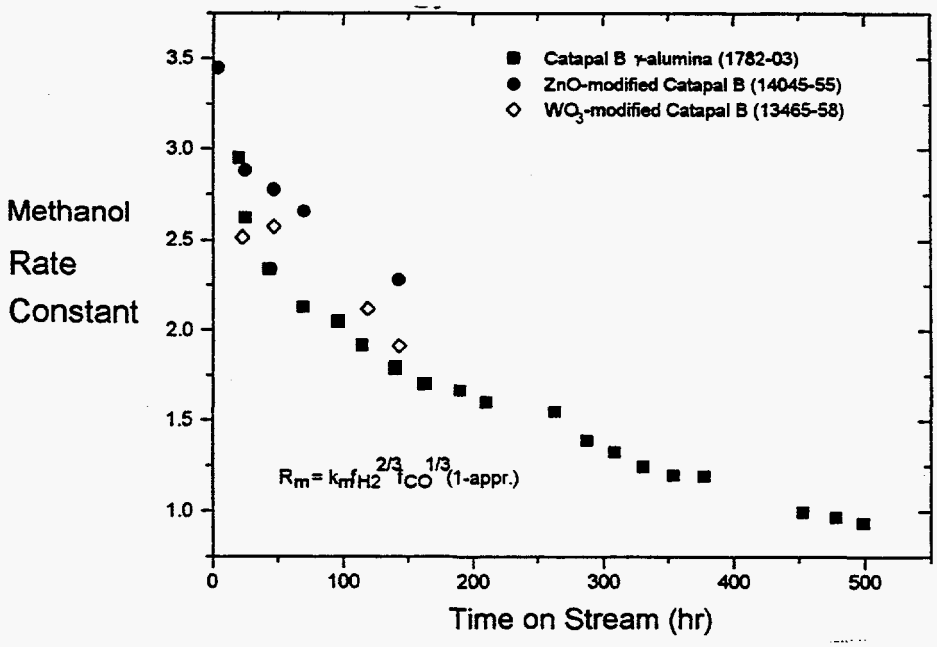

Figure 3.1.3. Dehydration Rate Constant as a Function of Time On Stream for Different Catalysts

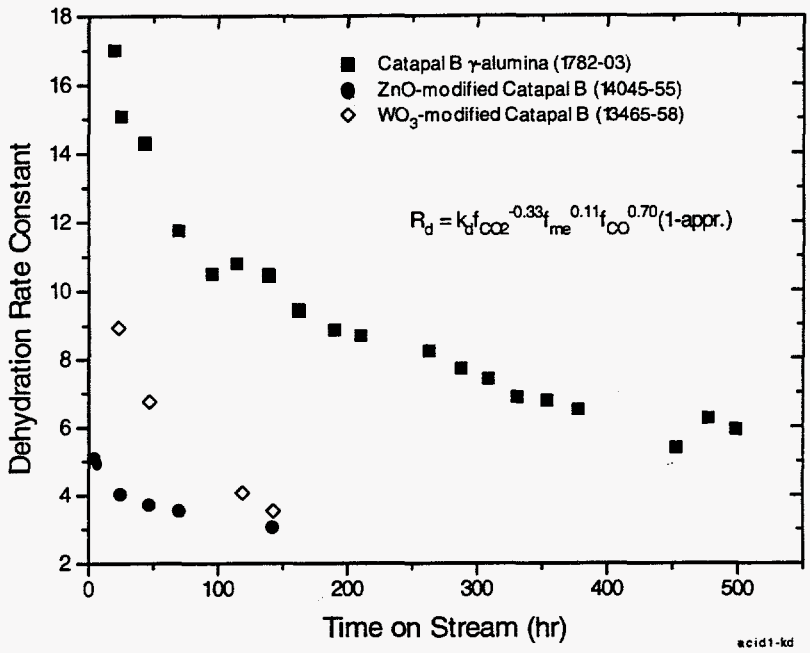

Fumed Alumina

Fumed alumina from Degussa (aluminum oxide C, average particle size = 13 nm) was tested along with BASF S3-86 methanol catalyst as an alternative dehydration catalyst (13465-91). Figure 3.1.4 shows that both initial methanol synthesis and methanol dehydration activities, in terms of rate constant, are low for this catalyst system as compared to the standard one, followed by continuous drop in both activities.

Figure 3.1.4. Activity of the Catalyst System Consisting of S3-86 and Fumed Alumina (13465-91)

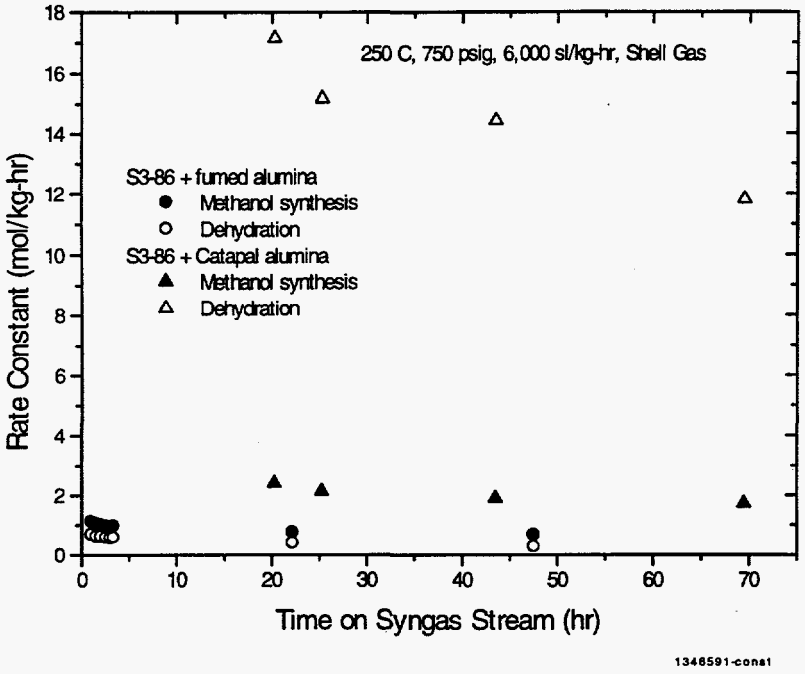

The interpretation of the poor activity and stability of this system is complicated by the following two factors. First, when the slurry was discharged from the reactor, clumps of the catalyst mixture were observed on the stirring rod and the walls of the reactor. This is due to low sedimentation of the very fine powders in the oil. If the sediment was also formed under the reaction conditions, it could lead to poor catalyst performance. The second complication is the fact that the fumed alumina contains a small amount of HCl (<0.5% by specification). The uncertainty is that Cl^- may migrate onto the methanol catalyst under the reaction conditions, leading to methanol catalyst deactivation, since Cl^- is a known methanol catalyst poison.

Metal Phosphates

Metal salts such as phosphates, sulfates, and chlorides have been used as industrial dehydration catalysts. Therefore, two phosphate samples were examined this month: one calcium phosphate, called hydroxyapatite, sample (Ca:P = 1.58), and a silica doped with 34% phosphorous acid. Owing to the high acid loading, the acid-doped silica contains some free H_3PO_4. Therefore, we would also like to use this sample to probe the possibility of using homogeneous acids as dehydration catalysts for LPDME. The runs were conducted under the standard LPDME conditions (250°C, 750 psig, 6,000 GHSV, 80:20 catalyst ratio). As shown in Figure 3.1.5, both samples have almost nil dehydration activity. This lack of activity could be due to the reaction temperature (dehydration using metal phosphates usually takes place at higher temperatures, e.g., > 300°C), the low water level in our system (high water level is needed to prevent H_3PO_4 from being dehydrated, therefore losing its acidity, above 200°C), or incompatibility with the methanol catalyst.

Figure 3.1.5. Dehydration Rate Constant as a Function of Time On Stream for Different Catalyst Systems

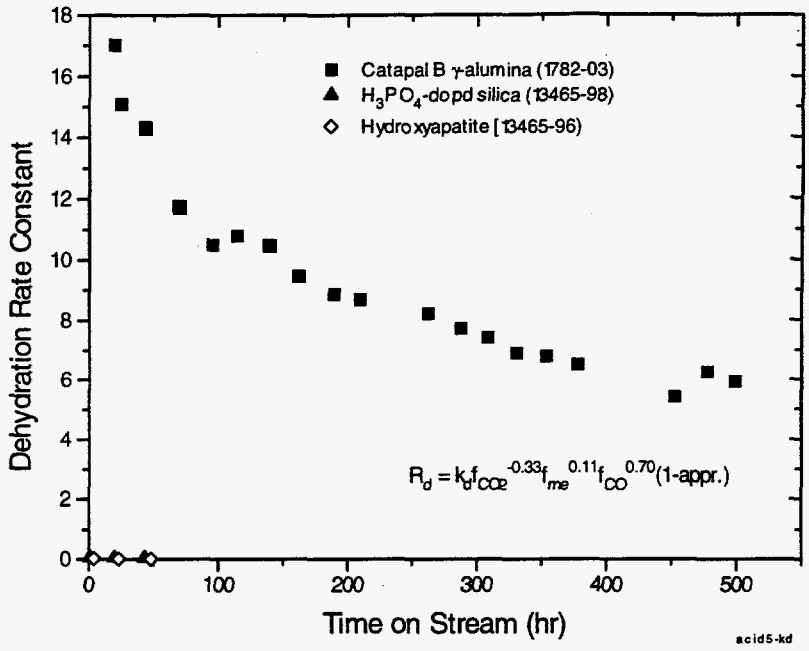

Figure 3.1.6. Methanol Synthesis Rate Constant as a Function of Time On Stream for Different Catalyst Systems

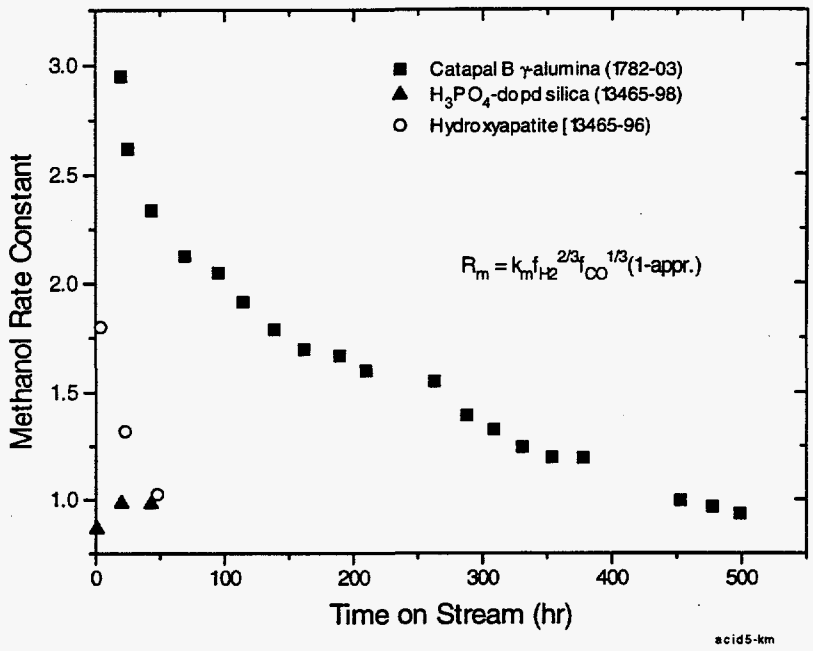

Both catalysts have significant impact on methanol catalyst activity, although they did not exhibit any dehydration activity. As shown in Figure 3.1.6, the methanol catalyst, when used along with the hydroxyapatite sample, deactivates at a higher rate than in the standard catalyst system. A different effect on the stability of the methanol catalyst was observed in the case of H_3PO_4-doped silica. The activity of the methanol catalyst must have been severely diminished during the reduction, as indicated by the low initial activity of the catalyst. The long-term impact of this sample on the methanol catalyst is not clear since the run was terminated at 43 hr on stream.

ZrO_2, and ZrO_2-Modified Silica Gel

Two ZrO_2-based materials were tested because dehydration of alcohols using ZrO_2 has been reported in the literature. A bulk ZrO_2 sample was obtained by calcining $Zr(OH)_4$ at 600°C for 6 hr. The surface area of the calcined sample was 38.1 m^2/g. The second sample, ZrO_2-modified silica, was prepared by impregnating a silica gel (Davison grade 55) with zirconium ethoxide, followed by calcination. Both test runs, conducted under the standard conditions (13465-88 and 14191-33), show that the ZrO_2 samples had essentially zero dehydration activity. While the bulk zirconia sample had little impact on the activity of the methanol catalyst, the ZrO_2-modified silica gel caused a continuous drop in the methanol catalyst activity.

Experiments using Robinson-Mahoney Basket Internals and Pelletized Catalysts

Robinson-Mahoney basket internals were purchased for our 300 cc autoclave from Autoclave Engineers Group. Figure 3.1.7 shows the assembly of this system. An annular basket, which sits

stationary inside the autoclave reactor, is used to hold pelletized catalyst samples. An agitator, connected to the shaft of our current reactor system, provides the necessary agitation. Baffles are built inside and outside the basket to prevent vortexing. This setup is designed to help understand the mechanism of catalyst deactivation under LPDME conditions. First, it enables us to separate spent methanol and dehydration catalysts for characterization. Second, it creates a physical environment different from the slurry such as pellets vs. powders, and there is an absence of collisions between catalyst particles. Whether this results in a different deactivation pattern will provide insight into the mechanism of catalyst deactivation.

Reactor Shakedown

A shakedown run of this reactor system was conducted using the BASF S3-86 methanol catalyst (#ZU 553-5072) alone. The catalyst pellets were between 1 and 3.35 mm. Before the run, the reactor system was passivated using flowing syngas at 300 C and 1,200 psig for 20 hr. The catalyst was reduced using the standard procedure. As shown in Figure 3.1.8, the standard heating ramp was too fast for methanol catalyst pellets in this setup, resulting in incomplete reduction; the total H_2 uptake during this reduction was 1.7 scf/lb, 61% of the normal uptake. The system was switched to Shell gas when the reduction temperature reached 240°C.

As shown in Figure 3.1.9, the methanol productivity of this system (9 mol/kg-hr) was much lower than that of a normal slurry phase run (15 mol/kg-hr). The apparent rate constant of this system was 70% smaller. The low activity was due to a mass transfer limitation in the system. Figure 3.1.10 shows that productivity increased with stirring speed. No attempt to overcome this limitation by exceeding 2,000 rpm was made because of potential damage to the system. The activity of the system appeared to be stable except for a small initial drop. However, it should be mentioned that the apparent activity of this system will not be sensitive to catalyst deactivation because the reaction rate is mass transfer limited.

The catalysts used in the LPDME run were BASF S3-86 tablets (#ZU 553 5072) crushed into a 1.0-1.7 mm size and Catapal B 1/8"x1/8" tablets from Calsicat (02E-60A) crushed into a smaller size (about four pieces from every tablet). The S3-86 and Catapal catalyst pellets were mixed first in a 80:20 ratio and loaded into the basket. Since the shakedown run showed much slower H_2 uptake by the pellets during reduction and incomplete reduction of the catalyst using the temperature ramp designed for powder S3-86, a new reduction scheme was employed in the current run, based on the BASF activation procedures for packed bed application. The reduction results are shown in Figure 3.1.11. Again, H_2 uptake was slower compared to the powder case. However, the final H_2 uptake (2.6 scf/lb) was close to the acceptable value (2.8 - 3.0 scf/lb), which is near the stoichiometric uptake.

Figure 3.1.7. Schematic of Robinson-Mahoney Stationary Catalyst Basket

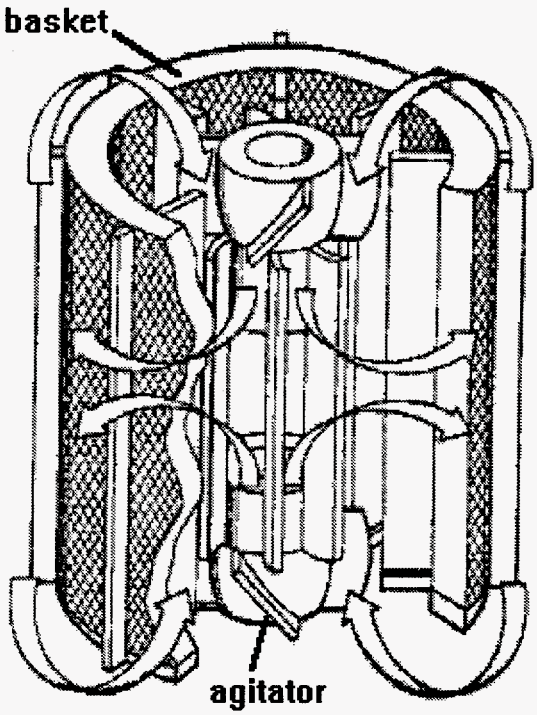

Figure 3.1.8. Profiles of Catalyst Reduction

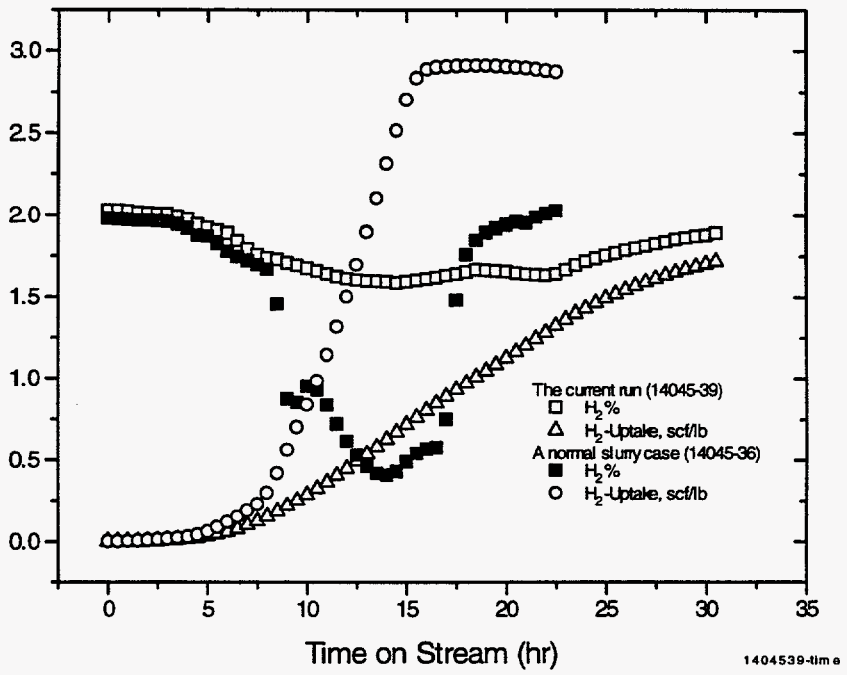

Figure 3.1.9. Shakedown Run of the 300 cc Autoclave with Robinson-Mahoney Basket Internals

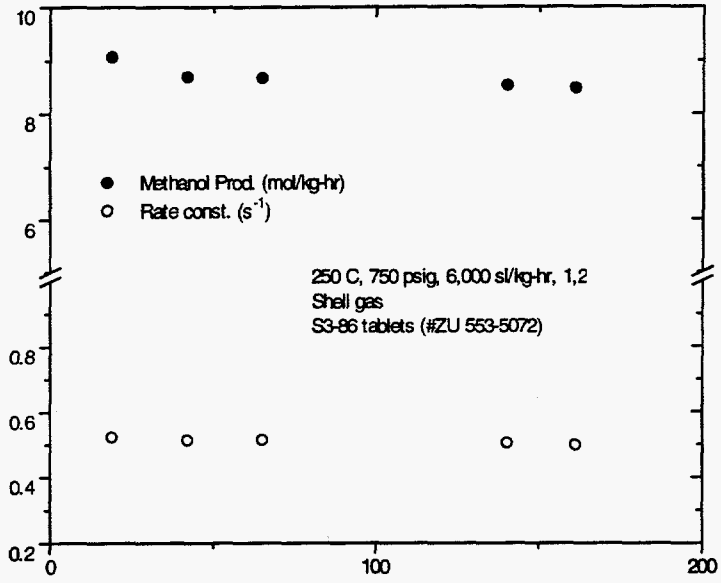

Figure 3.1.10. Activity as a Function of Stirring Speed

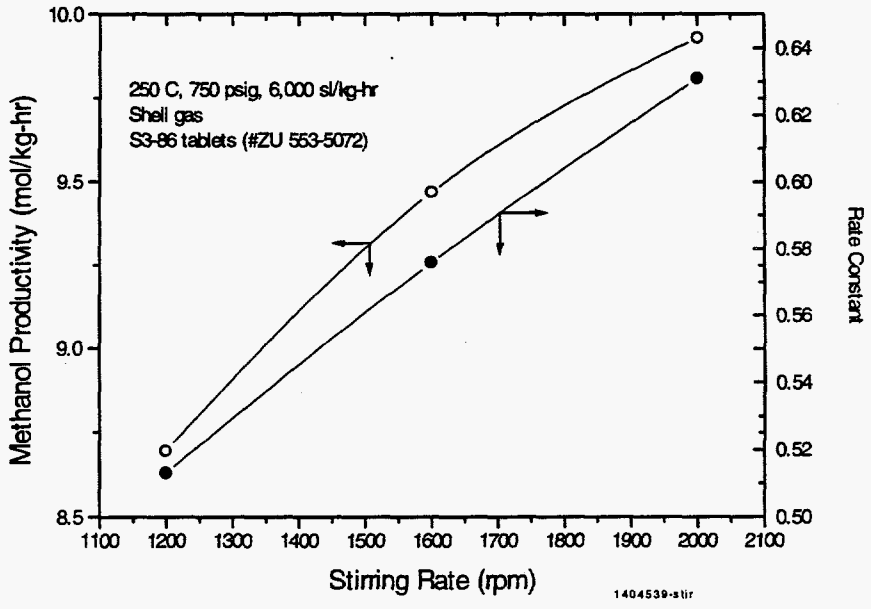

Figure 3.1.11. Reduction Profiles of the Robinson-Mahoney Run (10454-43)

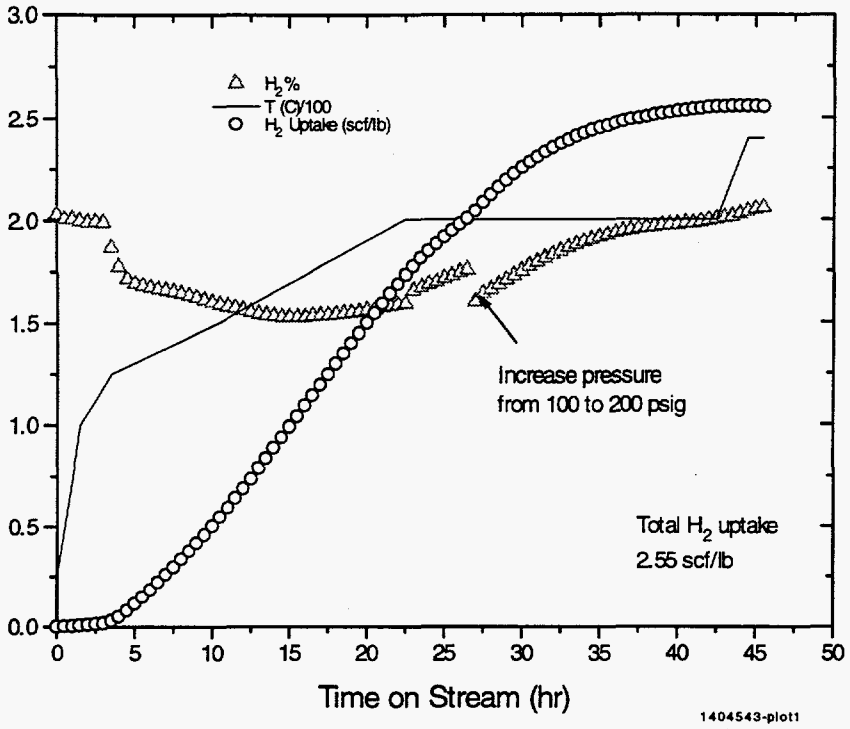

LPDME Run

The first part of the LPDME run was carried out at 250°C, 750 psig and 5000 GHSV using Shell gas. The stirring rate was higher than that used in slurry phase runs (1,600 vs. 1,200 rpm) to enhance mass transfer. As shown in Figure 3.1.12, the productivity of the system (10.5 mol/kg-hr) was only one third of the initial productivity (30 mol/kg-hr) of a mixture of S3-86 and Catapal alumina powders, indicating that the reaction was mass transfer limited. However, if the catalyst system deactivated, the reaction rate would eventually be comparable to the mass transfer rate, and from then on catalyst deactivation would be observable. The run was allowed to proceed for 350 hr more than needed for the reaction rate to slow down below the mass transfer rate, but no deactivation was observed. The stirring rate was then increased to 2,000 rpm to boost mass transfer rate, and space velocity was decreased from 6,000 to 1,500 sl/kg-hr to decrease the reaction rate, giving a better chance to observe catalyst deactivation. However, still little deactivation was detected up to 500 hr on stream.

Figure 3.1.12. LPDME Run Using Robinson-Mahoney Basket Internals (14045-43)

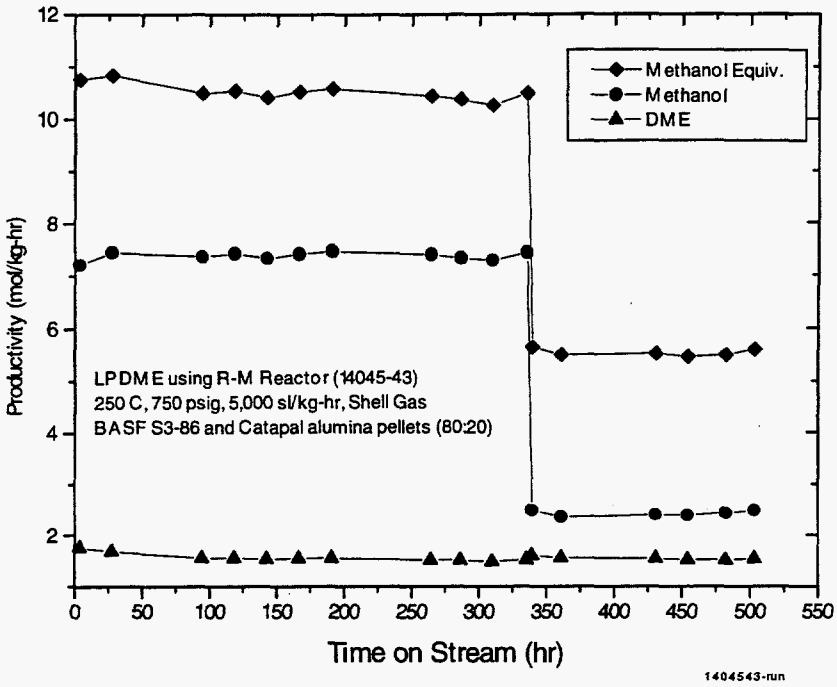

The run was stopped at this point. Part of the spent catalyst pellet mixture was preserved for analysis, and part was ground into powder in a nitrogen box and charged back in the autoclave reactor to check its activity. The reactor was operated in the slurry phase mode and free of mass transfer limitations. The powder mixture underwent the standard reduction. The minimal H_2 uptake, 0.17 scf/lb, occurred mainly between 100 and 130°C. The activity was checked under the standard conditions, and the results (14045-52) are summarized in Table 3.1.3.

Also listed in Table 3.1.3 for comparison are the activity data from two other experiments. The first one, 14045-58, was conducted using the powders prepared by crushing the *fresh* S3-86 and Catapal B pellets from the same batches used for the Robinson-Mahoney run. This measured the initial activity of the catalyst system used for the Robinson Mahoney run. The second experiment (11782-3) was a standard LPDME life run using genuine powder samples. As shown in Table 3.1.3, the S3-86 powder prepared from the fresh S3-86 pellets had the same activity as the genuine S3-86 powder. The dehydration activity of the Catapal B powder prepared from the fresh pellets was only slightly lower (11%) than that of the genuine Catapal B powder.

Table 3.1.3. The Activity of the Catalysts used in the LPDME Run using Robinson-Mahoney Basket Internals. Reaction conditions: 250°C, 750 psig, 6,000 sl/kg-hr, Shell Gas

Run	Catalyst	Time on Stream, hr	MEOH Equiv. Prod. (mol/kg-hr)	Concentration (%) MEOH	DME	Rate Constant k_m[b]	k_d[c]
14045-52	powders from spent pellets	508	27.1	1.53	5.96	2.7	10.2
14045-58	powders from fresh pellets	20.5	30.6	0.78	7.06	2.9	15.1
11782-03	genuine powders	20	30.7	1.01	6.95	3.0	17.0
"	"	499	14.0	0.49	2.67	0.9	5.9

a: Methanol synthesis rate constant calculated from $R_m = k_m k_{co_2} f_{H_2}^{2/3} f_{CO}^{1/3} (1 - appr.)$, based on methanol catalyst weight.

b: Methanol dehydration rate constant calculated from $R_d = k_d f_{CO_2}^{-0.33} f_{MEOH}^{0.11} f_{CO}^{0.70} (1 - appr.)$, based on alumina weight.

The results in Table 3.1.3 indicate that 500 hours in the Robinson-Mahoney run did not cause a significant change in the methanol catalyst activity (a 7% drop). For a similar period in the normal LPDME life run in a slurry phase reactor (11782-3), a much greater drop in activity was observed (70%). In fact, the activity of the methanol catalyst pellets dropped at a rate of only 0.013% hr^{-1} in the Robinson-Mahoney run. This rate is even smaller than the S3-86 powder under LPMEOH conditions in a 300 cc autoclave (0.045% hr^{-1}).

However, deactivation in the dehydration catalyst was observed in the Robinson-Mahoney run. The Catapal B pellets lost 32% of their activity upon 508 hours on stream. From this single experiment, there is no way to tell if this deactivation occurred only in the early period of the run or throughout the run. Note that in the normal LPDME life run (11782-3), the dehydration activity dropped by 65% in a similar period.

This experiment shows two important phenomena:

1) Point contact between methanol catalyst and alumina *pellets* does not cause deactivation of the methanol catalyst.
2) The fluid phase (mineral oil) neither causes nor transports anything that causes deactivation.

This suggests that certain physical features in a slurry phase operation, such as attrition which leads to the formation of methanol catalyst and alumina fines and good mixing between two catalyst powders, may be the cause or a necessary step for methanol catalyst to deactivate. For instance, these features may provide large contact area and long contact time, which are needed to foul the methanol catalyst or to go through solid phase reactions between methanol catalyst and alumina.

In contrast, the physical features associated with a slurry phase operation are not necessary for the alumina catalyst to deactivate. If one assumes that this deactivation is caused by migration of

Cu- and/or Zn-containing species from the methanol catalyst to the alumina, then this migration is conducted either by surface diffusion through the point-contact between the pellets of the two catalysts or mass transfer through the fluid medium, or both. More severe deactivation in dehydration activity occurred in the powder case for a similar period (Table 3.1.3), indicating that either this process can be accelerated by good mixing in a slurry phase operation, or there exists an additional mechanism for alumina deactivation, e.g., a process in concert with the deactivation of the methanol catalyst. In addition to this migration hypothesis, coking could be the cause of alumina deactivation. Elemental and coke analysis of the spent alumina sample will be conducted to resolve this issue.

3.2 New Fuels from Dimethyl Ether (DME)

Overall 2QFY95 Objectives

The following set of objectives appeared in Section III of Quarterly Technical Progress Report No. 1 (Oct 94 - Dec 94).

(i) Continue to develop the concept of methanol to isobutanol over compositions of Ag, Cs/SrO with the goal of increasing oxygenate selectivity.

(ii) Prepare DME carbonylation catalyst candidates for immobilization on supports.

(iii) Initiate catalyst development work on the cracking of ethylidene diacetate to vinyl acetate and acetic acid.

(i) Chemistry and Catalyst Development

Methanol to Isobutanol

The Ag/K/SrO catalyst was retested to check reactor performance. The catalyst deactivated quickly, as in the sample tested and reported in the last quarterly. Carbon balances from the on-line GC averaged 84%. By method of preparation, the Ag and K wt % values were 6.6 and 8.2, respectively.

The Ag/Cs mol ratio was then varied as shown in Table 3.2.1. The weight % of Ag and the weight % of Cs are represented by x and y, respectively. Catalyst #1 was reported in the last quarterly and produced a mol % selectivity to C_2-C_4 oxygenates of ~23-17. Catalyst #2 was stopped after ~45 hours of testing, and the oxygenate selectivity was ~15-12 mol %. Oxygenate selectivity was lower than that for Catalyst #1, but the activity was constant. Catalyst #3 was stopped after 70 hours of testing because the oxygenate selectivity dropped from 12-5 mol %. The data suggest that when the mol ratio of Ag/Cs is ~1, or possibly less than 1, the catalyst is more selective for C_2-C_4 oxygenate and has a reasonable lifetime.

The best catalyst, catalyst #1, was prepared again to determine reproducibility of the catalyst preparation procedure. The conversion - selectivity profile is shown in Figure 3.2.1. The near constant selectivity is similar to that reported before. The only difference is the volume of

catalyst charged. At 2 ml of catalyst charged, the methanol conversion nearly doubled while the oxygenate selectivity remained nearly the same.

The Ag/Cs ratio of 0.5 on SrO, catalyst 4, was prepared and tested. The mol % selectivity to useful oxygenates was 12-15% conversion. Carbon mass balances were in the 91-109 % range. To date the best Ag/Cs ratio is ~ 1.

Table 3.2.1 x%Ag; y%Cs on SrO

Cat.	x	y	x/y	mol % useful oxygenates*	hrs. on-stream
1	5.8	7.3	1.0	23-17	200
2	7.0	4.4	2.0	15-12	45
3	10.9	4.1	3.0	12-5	70
4	3.4	8.4	0.5	15-12	80

*Ethanol + Propionaldehyde + Isobutyraldehyde + n-Propanol + Isobutanol

Figure 3.2.1. Methanol Conversion and Ethanol + Propionaldehyde + Isobutyraldehyde + n-Butanol + Isobutanol Selectivity vs Time on Stream

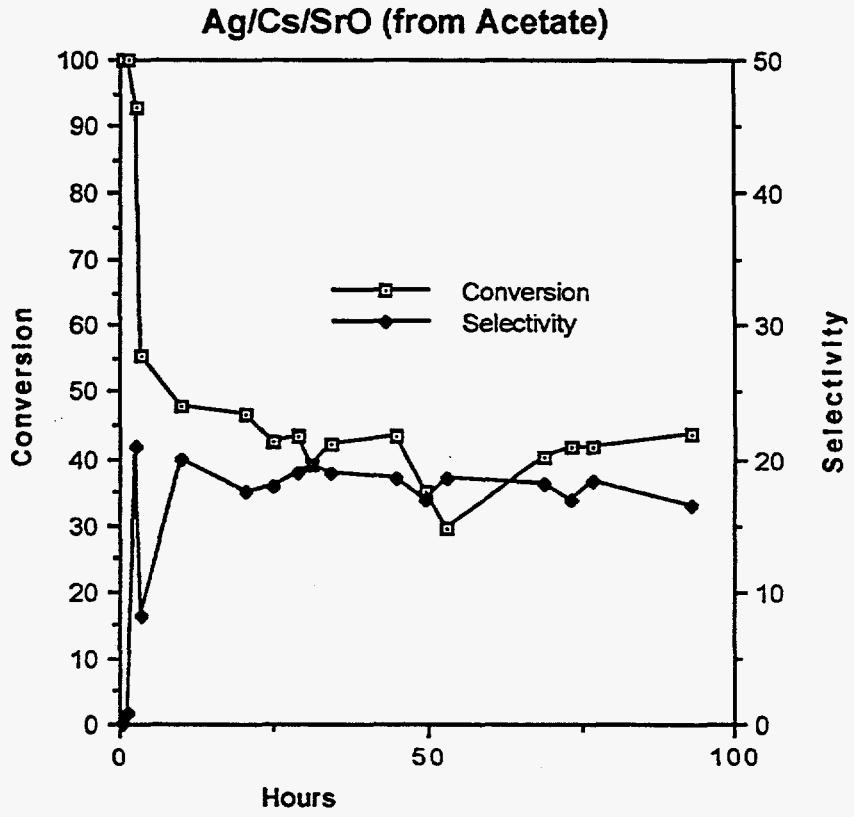

The Ag and Cs were supported on MgO with a mol ratio of 1. The wt% Ag and Cs were 5.8 and 7.3, respectively, based on method of preparation. The conversion and selectivity plot is provided in Figure 3.2.2. The mol % to useful oxygenates was 5%. Since the methanol conversion was decreasing, the run was terminated. Carbon mass balances were in the 83-87% range.

Figure 3.2.2. Methanol Conversion and Ethanol + Propionaldehyde + Isobutyraldehyde + n-Butanol + Isobutanol Selectivity vs Time on Stream

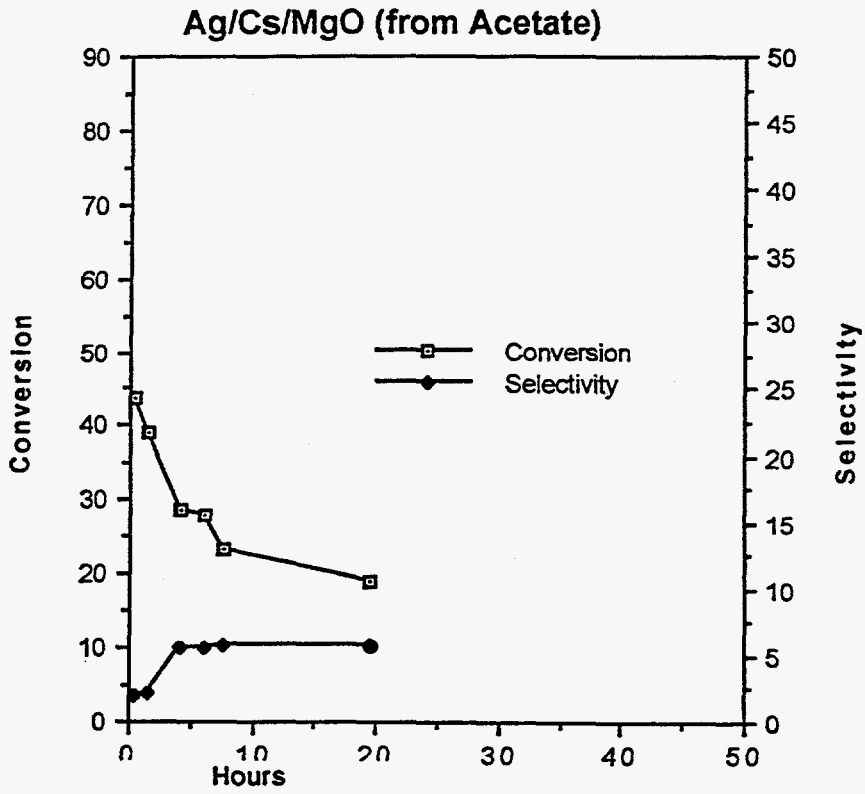

Similar results were obtained by supporting Ag and Cs on CaO when the ratio of Ag/Cs was 1. Figure 3.2.3 illustrates the steady decline in methanol conversion and oxygenate selectivity. Carbon mass balances were in the 70-91% range.

Figure 3.2.3 Methanol Conversion and Ethanol + Propionaldehyde + Isobutyraldehyde + n-Butanol + Isobutanol Selectivity vs Time on Stream

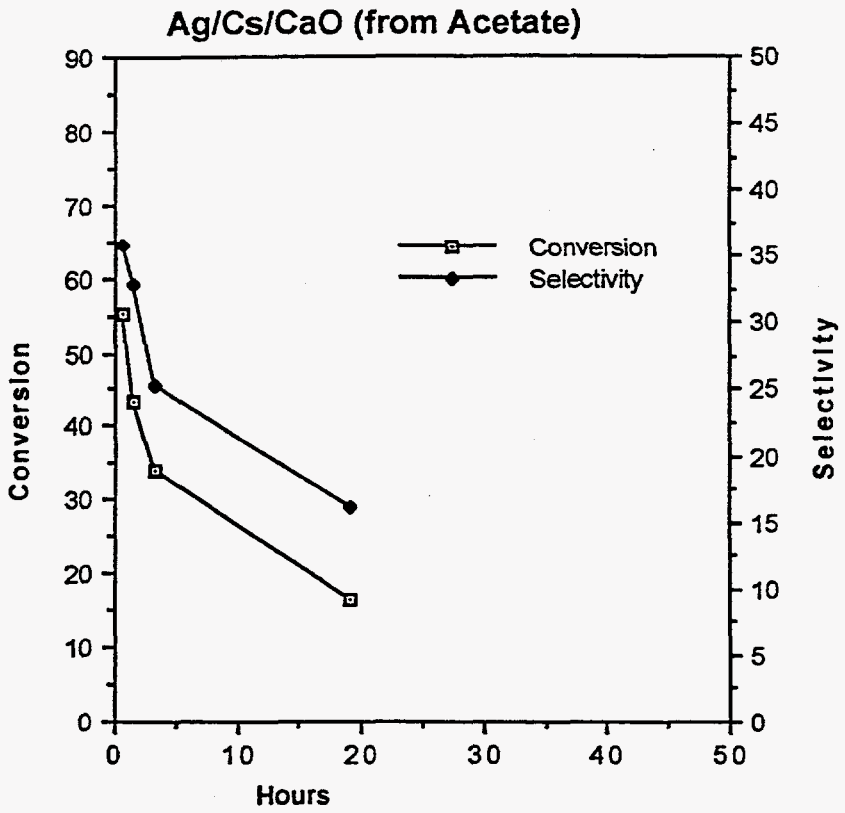

However, with a change of the Ag/Cs ratio to 0.5, the oxygenate selectivity increased with time (Figure 3.2.4). This catalyst will be re-tested. The carbon mass balances were in the 85-90% range.

Figure 3.2.4. Methanol Conversion and Ethanol + Propionaldehyde + Isobutyraldehyde + n-Butanol + Isobutanol Selectivity vs Time on Stream

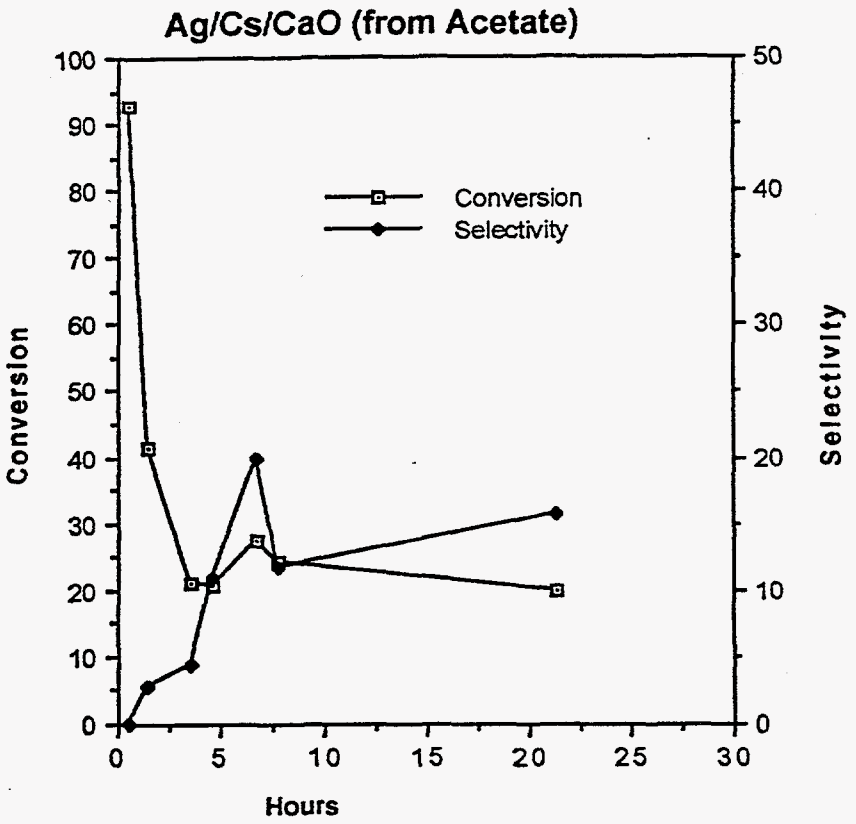

Ag and Cs are currently impregnated onto the SrO together from the same solution as the acetate salts. One synthetic variation is to impregnate the SrO first with Cs, followed by calcination treatment, and then to impregnate with Ag. This yields a catalyst that performs like the regular preparation procedure. Carbon mass balances were 90+%.

(ii) DME to Ethylene Diacetate (EDA)

Literature Review

In early January, a literature search was conducted on heterogeneous carbonylation catalysts, and based on this search, a plan was generated for our goal of converting DME to EDA.

One approach is to prepare a rhodium complex supported on an anion exchange resin in order to generate the catalytically active $[Rh(CO)_2I_2]^-$ for carbonylation. The three important patents in this area are those of Drago et al. (US 4328125), Marston et al. (US 5155261), and Minami et al. (US 5364963). All of these patents deal with heterogeneous catalysts for the conversion of methanol to acetic acid. For example, Drago et al. have taught a way to prepare a rhodium catalyst supported on a polystyrene vinylpyridine copolymer via the scheme shown below.

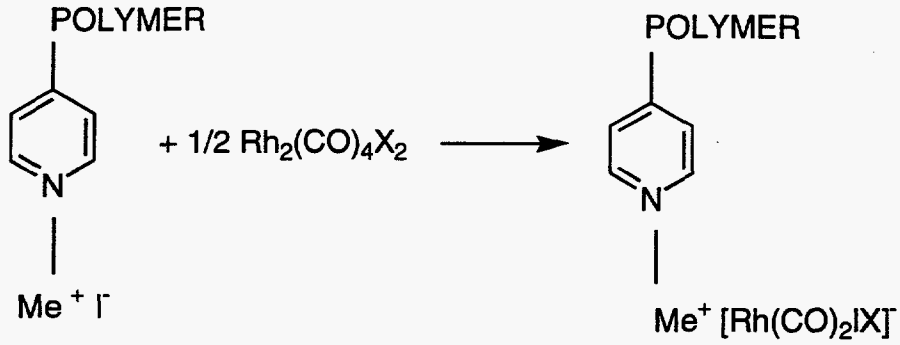

This method involves first refluxing the polymer with methyl iodide, followed by a reaction with the rhodium carbonyl. The same catalyst could also be prepared in the reactor by using $RhCl_3.XH_2O$ with commercially available resins such as Amberlite IRA-400 or Dowex 1-X8 resins.

Luft et al. (Chem.-Ing. Tech., Vol. 59, 1987, pp. 485-486) have prepared cationic phosphine complexes of rhodium such as $[Rh(dpe)_2]^+BF_4^-$, dpe=diphenylphosphinoethane, which they have supported on alumina, silica and activated charcoal. These have been used for the gas phase carbonylation of methyl acetate to acetic anhydride using a feed of CO/methyl acetate/methyl iodide at a pressure of 11 bar, 185°C. The same catalyst was also observed to convert DME to acetic anhydride in the gas phase, though the conversion was much slower (lower by a factor of 4).

The most important patents for the preparation of EDA from methyl acetate by using a heterogeneous Rh catalyst are those of Park et al. (US 5371274, US 5371275). The first patent uses the catalyst $RhClCO(PPh_3)_2$ supported on a carrier like alumina, keiselguhr, or silica, together with an accelerator such as triphenylphosphine. The reactants are methyl acetate,

iodomethane, CO, H_2, where the molar ratio of CO to H_2 varies from 1:1 to 1:6. The reaction is conducted as a continuous process at a temperature between 90-250°C and a pressure between 20-70 atmospheres. From the analytical data shown, there appears to be a greater yield and selectivity towards acetic acid. The second patent shows a way of supporting the same catalyst on a phosphinated DVB-PS resin as shown by the reaction scheme below.

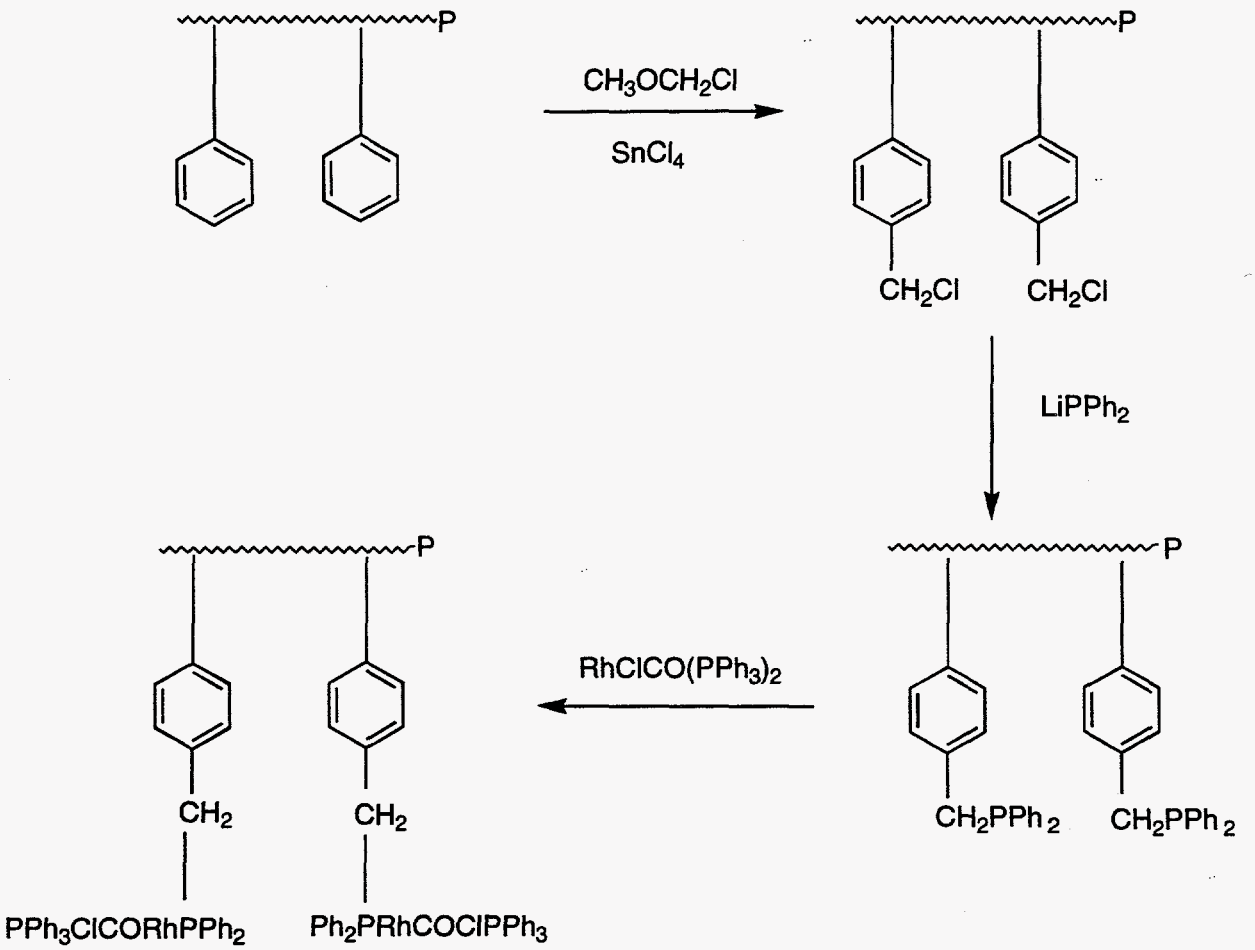

An accelerator such as 3-picoline was added to facilitate the catalytic reaction. The feed gases and reaction conditions were the same as those used for the alumina supported catalyst, and though EDA was produced, acetic acid was a major product.

Catalyst Preparation and Characterization

A sample of Reillex 425 polymer was obtained from Reilly Industries. This polymer is made by crosslinking 4-vinylpyridine with divinylbenzene, and is available as off-white beads that are thermally stable up to 260°C. The beads as obtained are wet, with a water content of 50-60%. Approximately 24g of the Reillex 425 were dried in a regular oven at 90°C for 12 h. To these beads were added ~125ml of toluene, and the mixture was refluxed for 30 min. under nitrogen. The beads were observed to expel the trapped air and then sink to the bottom of the flask. After the mixture cooled to room temperature, 20 ml of methyl iodide were added, at which time the

beads were observed to turn pale yellow. The solid was filtered and dried under vacuum. The actual reaction is described by the equation shown below.

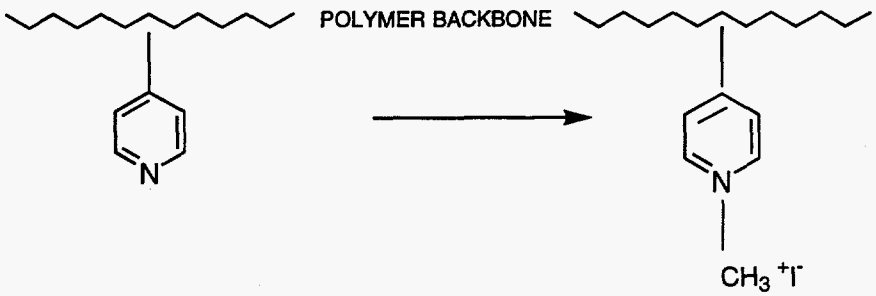

The solid was characterized by solid state ^{13}C nmr. The spectrum of the Reillex 425 shows a strong signal at 40 ppm due to the hydrocarbon backbone of the polymer. After the reaction with methyl iodide, the spectrum shows a new shoulder at 50 ppm due to the methyl group on the pyridine. Also it can be seen that the aromatic carbons at 130 and 150 ppm are shifted closer together. This is further evidence that the nitrogen on the pyridine has been alkylated. However, it does not tell how many free pyridines are left over at the end of the reaction.

The next step of the reaction was to load the Reillex polymer with a rhodium complex by the reaction shown below:

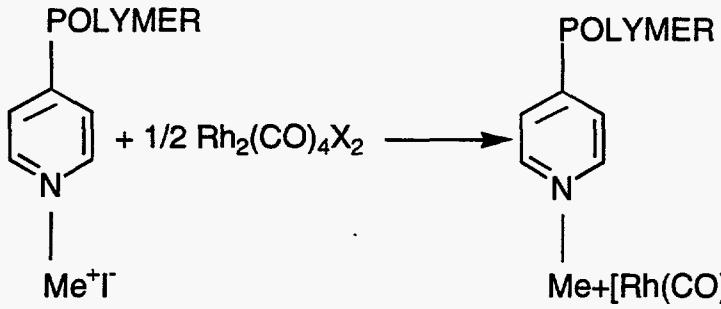

Approximately 4g of the alkylated Reillex were added to a solution of 0.18g $Rh_2(CO)_4Cl_2$ in 100 ml of toluene. Immediately, the yellow color of the solution dissipated and the yellow Reillex became more orange. If all of the rhodium incorporated, this would amount to a 2.375% loading. However, the actual loading can only be found by an elemental analysis. An infrared spectrum of the solid now showed two characteristic carbonyl bands at 2056, 1983cm^{-1}, which corresponds well with the literature values of the tetraphenylarsonium $[Rh(CO)_2I_2]$ at 2060 and 1988cm^{-1}.

Catalyst Testing

The catalytic performance of the heterogeneous catalyst was compared with the analogous homogeneous system using similar experimental conditions (syn gas, 190°C, 1500 psi).

Test 1 - Homogeneous Catalysis Without Lithium Iodide
Reaction conditions were 0.2 g $RhCl_3.3H_2O$, 8.13 g DME, 9 g methyl iodide, 143.7 acetic acid, syn gas (50:50), 190°C, 1500 psi. The results are shown in Figure 3.2.5.

Figure 3.2.5. Hydrocarbonylation of DME with a Homogeneous Rhodium Catalyst without LiI

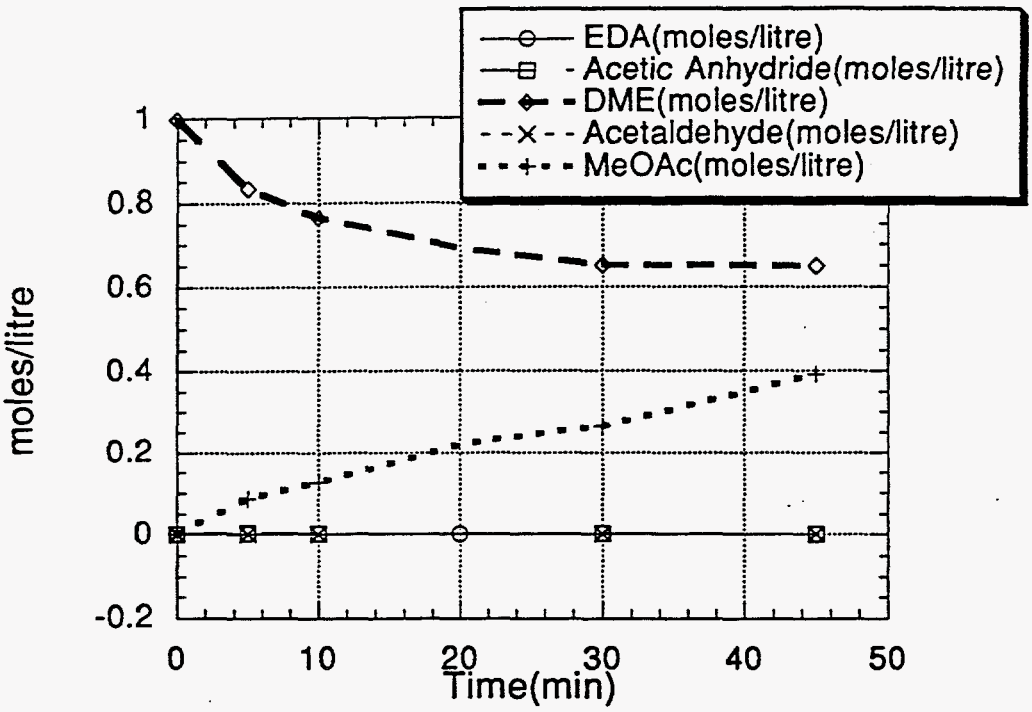

It can clearly be seen that over a period of 45 min. the DME concentration decreases while the methyl acetate concentration builds up. However, no products in the form of acetic anhydride, acetaldehyde or ethylidene diacetate were seen.

Test 2 - Heterogeneous Catalysis Without Lithium Iodide
Reaction conditions were 1.47g Reillex containing 2% Rh, 10.87g DME, 9g methyl iodide, 145.46g acetic acid, syn gas (50:50), 190°C, 1500 psi. The results are shown in Figure 3.2.6.

Figure 3.2.6. Hydrocarbonylation of DME with a Heterogeneous Rhodium Catalyst without LiI

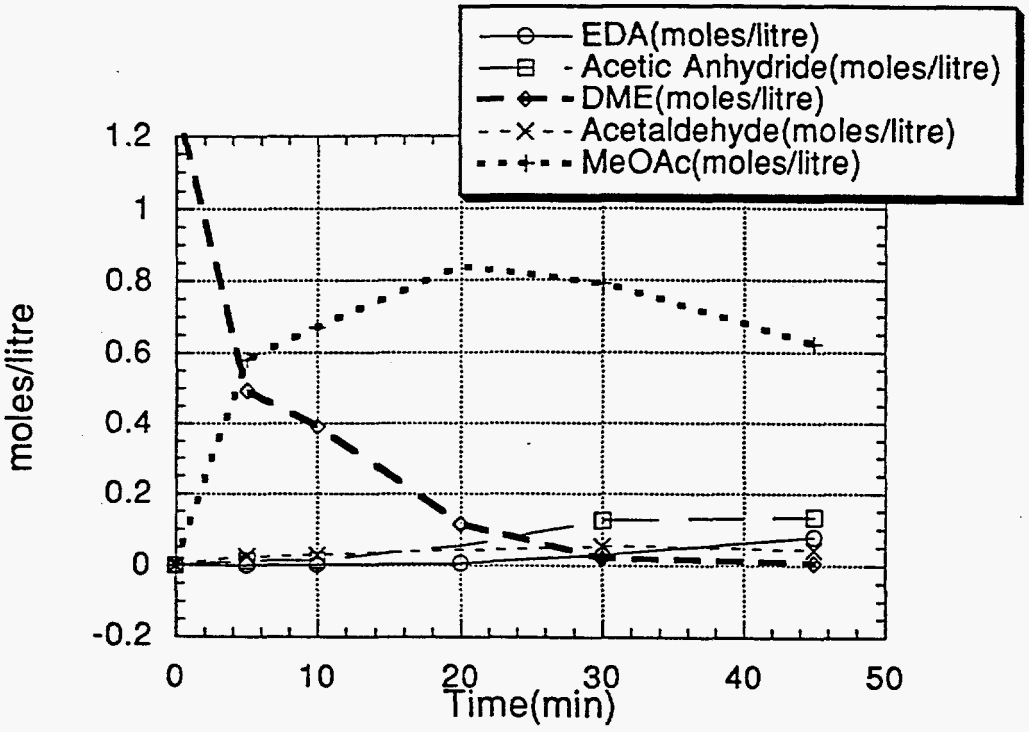

It can clearly be seen in the plot shown above that the heterogeneous catalyst behaves much better than the homogeneous one (test 1). The DME concentration drops rapidly and is almost completely consumed by the end of 45 minutes. The methyl acetate concentration builds up until the 20 min. mark, after which it drops presumably because the carbonylation rate now exceeds the rate of formation. The time axis also shows that between the 30 and 45 minute mark, a significant concentration of products (acetic anhydride, acetaldehyde, EDA) is seen.

At the 5 minute mark, the acetaldehyde concentration is higher than the acetic anhydride concentration. This must mean that there is another mechanism for the formation of acetaldehyde directly from methyl acetate, in addition to the expected conversion of acetic

anhydride to acetaldehyde via hydrogenation. At the 20 minute mark we see the first signs of product EDA, and this rises steeply up to the 45 minute mark. Both the rates of formation of acetaldehyde and acetic anhydride are observed to decrease at the 30 minute mark, presumably because they are reacting together to form the product EDA.

The catalyst sample was analyzed for rhodium before and after the catalytic run to see if there was extensive leaching of the catalyst. The sample before the test run gave a 2% Rh analysis, while the sample after the test run gave a 1.63% Rh analysis. Based on these results we do not feel that there has been extensive leaching of the catalyst. The small difference in analysis may simply be due to further incorporation of methyl iodide into the polymer via reaction with pyridine groups, which will increase the weight of the polymer and reduce Rh analysis slightly. We plan to further test this hypothesis by doing successive catalytic runs using the same batch of material.

Test 3 -Heterogeneous Catalysis With Lithium Iodide

Reaction conditionswere the same as those for Test 2, except that 1.5g of LiI was added. The results are similar to those obtained with Test 2, and the added LiI did not show any advantage. In fact it proved to be a disadvantage as we observed major leaching of catalyst from the polymer. The Rh analysis was 0.55% after the run compared to 2% before the run. This is not unexpected since the iodide ions from the LiI could exchange with the anionic Rh complex.

Test 4 - Homogeneous Catalysis With Lithium Iodide

Reaction conditions were 0.2g $RhCl_3.3H_2O$, 9.9g DME, 9g methyl iodide, 1.49g LiI, 0.81g LiOAc, 146.8g acetic acid, syn gas(50:50), 190°C, 1500 psi. The results are shown in Figure 3.2.7.

Figure 3.2.7. Hydrocarbonylation of DME with a Homogeneous Rhodium Catalyst with LiI

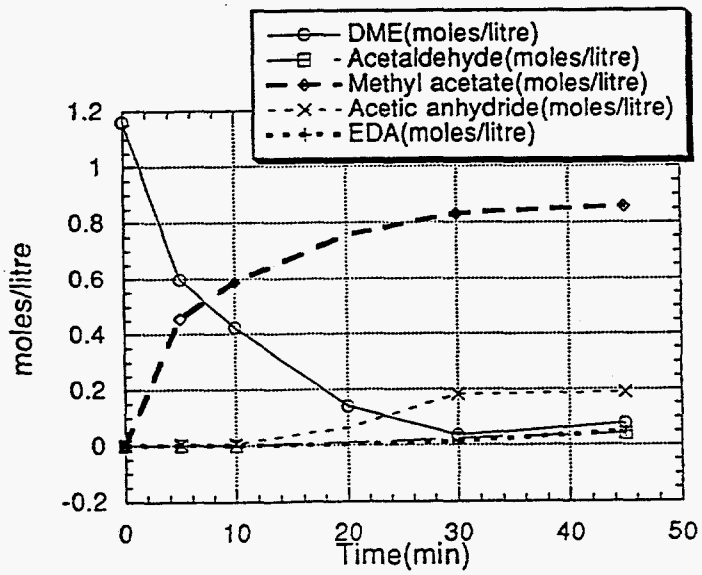

The addition of LiI and LiOAc to the homogeneous reaction does make the product EDA in contrast to Test 1, where no product was obtained. However, this reaction does not work as well as the heterogeneous reaction (Test 2), even though the homogeneous reaction yielded twice the amount of Rh by weight.

(iii) Nothing to report this quarter.

3Q FY95 Objectives

Future plans for Task 3.2 will focus on the following areas:

- Continue to screen immobilized catalyst candidates for hydrocarbonylation of dimethyl ether to ethylidene diacetate
- Determine the extent of any catalyst leaching from the best candidate
- Initiate catalyst development work on the cracking of ethylidene diacetate to vinyl acetate and acetic acid.

3.3 New Processes for Alcohols and Oxygenated Fuel Additives

3.3.1. Isobutanol Synthesis in a Three Phase System (RWTH Aachen)

Fixed Bed Reactor Design and Runs

The results from the fixed bed reactor were improved compared to those of the last quarter, paralleling the results reported by Falter. These results are provided in Figure 3.3.1.1:

Figure 3.3.1.1 Results from Catalytic Tests in the Fixed Bed Reactor

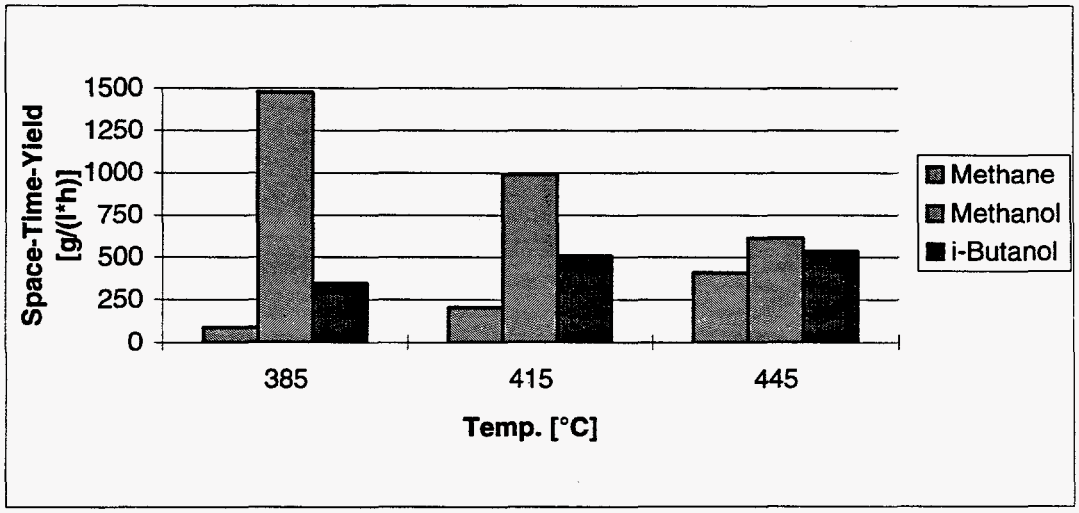

Pressure: 25 MPa
GHSV: 20000 h^{-1}
Catalyst: $ZrO_2/ZnO/MnO/K_2O/Pd$ (pH 9)

These improvements were achieved by changes in catalyst synthesis and the reduction of catalyst poisons. Former catalytic tests revealed a significant activity towards methane. These unexpected results led to the investigation of the presence of catalyst poisons. Surface analysis of catalyst pellets after reaction by x-ray fluorescence indicated iron and nickel impurities. In contrast, fresh catalysts were free of these impurities.

Consequently, the syngas was checked for iron pentacarbonyl by IR and indeed showed the expected peaks. The filter material used, a 4Å molecular sieve, was not able to adsorb iron pentacarbonyl. By using activated carbon as the filter material, the space time yield to methane was reduced more than ten times with respect to former runs. Since activated carbon was used as the filter material, the fixed bed results were improved and the influence of the temperature gradient at the reactor top was diminished. Best results were found without a temperature gradient.

It was observed that the reactor itself set nickel and iron free by corrosion. The roughness-height of the fixed bed reactor was considered to be the cause. Instead of reaming the fixed bed reactor used to date, a new reactor was made with a very smooth inner surface. A comparison between this new reactor and the one used by Falter showed quite similar results for isobutanol and methanol; in addition methane production in the new reactor was reduced another 50%.

Slurry Reactor Design and Runs

Two runs under the same reaction conditions were made using the slurry reactor, which could be connected to the unit without other modifications. On-line GC, product sampler and process management systems were run as if the fixed bed reactor would be used. The results from the slurry reactor can be compared directly to those obtained with the fixed bed reactor. The reaction conditions are listed in Table 3.3.1.1:

Table 3.3.1.1 Reaction Conditions for the Slurry Reactor

Temperature	400°C
Pressure	25 MPa
Mass flow	100 Nl/h (Syngas)
Catalyst	8 g powdered BASF "Isobutylölkatalysator"
Inert liquid	200 ml Decalin
Number of revolutions	1000 rpm

Methanol production was halved compared to the fixed bed reactor. Isobutanol production was about six times smaller. Decalin was found to be stable. It should be mentioned that these initial runs mainly served to check the unit's characteristics.

Due to the high vapor pressure of decalin, a complete separation of decalin and the reaction products in the reflux condenser seems impossible. Within 40 hours the amount of decalin in the reactor decreased. It seems necessary to recirculate the decalin after phase separation using a high pressure pump.

Future objectives are optimization of the slurry reactor and further tests with the catalysts mentioned under slurry conditions.

On-Line Screening

For injecting the samples without pressure, a different gas switching mode was designed. A better reproducibility of the of the on-line results has thus been achieved. In this way the maximum error has been minimized to a value smaller than 5%.

Catalyst Preparation

To improve the knowledge of the $ZrO_2/ZnO/MnO/M_2O/[Pd]$ (M: Li, K)[1] -type catalysts, one main objective has been the analysis of these catalysts. For this purpose they have been investigated using the following methods[2]:

***AAS/XRF*:** The quantitative analysis by AAS was inaccurate because the measurement of zirconium is influenced by potassium. Nevertheless, this analysis showed that the samples precipitated with potassium at pH 9, 10 and 11 (BJ 27, 26, 31) were identical in their zinc and manganese content, but different in their potassium content. The calibration of the XRF-spectrometer has almost been completed. First results confirm the similarity in zinc, manganese and zirconium content.

***Nitrogen Adsorption*:** The determination of BET- surfaces and porous structures showed surfaces of ca. 130 m^2/g and porous maxima in the range of 40-80 Å for all samples. Nitrogen adsorption has not yet been measured for palladium impregnated catalysts.

***XRD*:** All catalysts were mainly amorphous. The observed crystalline phases were absolutely similar. So far these phases seem to be $Zn_2Mn_4O_8 \cdot H_2O$ (Hydroheterolyte), $ZnMn_2O_4$ (Heterolyte), $Zn(OH)_2$ (Ashoverite), Mn_3O_4 (Hausmannite) and Zn_2MnO_4. No crystalline phases of pure zinc- or manganese-oxides and only very small amounts of crystalline zirconium oxide could be identified.

***DSC/TG*[3]:** In correspondence with the results mentioned, the thermogravimetric analysis revealed similar characteristics for the different catalysts, showing a slow loss of capillary- and surface water up to a temperature of 450-500°C and an exothermic effect without mass-loss (probably a phase transformation of zirconium oxide) at 650-690°C.
Typical examples of the analysis data are depicted in the appendix.

Conclusions drawn from these results are as follows:

- A precipitation pH ranging from 9-11 does not seem to affect the composition (excluding the alkaline content), surface, porous structure and crystallinity of the $ZrO_2/ZnO/MnO/M_2O$ (M: Li, K)- catalysts.

---

[1]All catalysts were calcined in flowing air at 330°C, with a heating rate <5°/min.

[2]Analysis has been completed for the potassium-containing catalysts. The results from the lithium-catalysts so far obtained confirm all statements.

[3]DSC / TG measurements have been made from the dried (130°C) but uncalcined catalysts

- Conclusions concerning the composition of the amorphous phases and the oxidation states of the transition metals cannot be drawn.
- So far the only perceivable difference between these catalysts is the alkaline content. This observation could be related to the differences in catalytic behavior.

Coprecipitated Alkaline Free Catalysts

The most direct way of studying the influence of alkaline metals in the Falter system is a precipitation followed by a washing procedure and subsequent impregnation. This can be done by washing with distilled water and measuring the conductivity of the washing water. As a first step, alkaline-free catalysts based on the precipitation with potassium hydroxide at pH 9 and 11 were prepared. Analysis showed absolute similarity to the alkaline-containing samples.

These catalysts will be impregnated with defined amounts of potassium acetate, calcined a second time and tested in catalysis. First, this will enable us to investigate whether there is any influence introduced through coprecipitation at different pH-levels. Similar behavior in catalysis after impregnation with the same amounts of potassium would confirm the analytic results. Second, this provides a way to optimize catalysts concerning their alkaline content.

Falter also obtained excellent results with catalysts prepared from different first and second main group metal bases. Therefore the following tests would be interesting if the above mentioned experiments are successful:

- Impregnation with different first and second main group metals instead of potassium in order to compare the influence of different bases.
- Precipitation with different first and second main group bases at several pH values, followed by washing them alkaline free. These catalysts could be impregnated with the same alkaline base to clarify whether the major influence of the alkaline base is exerted during precipitation or only by the absolute amount present.

Impregnation with $Pd(acac)_2$

The impregnation step with $Pd(acac)_2$ in acetonitrile was pointed out by Falter to increase both activity and selectivity to isobutanol. This impregnation step is performed by using a static impregnation method, leaving the catalyst pellets in an acetonitrile solution (30 ml) of $Pd(acac)_2$ (2.5 mg Pd/g catalyst). After decoloration of the yellow solution (3-14 days), the catalyst is filtered from the solution and calcined. In the case of catalysts $ZrO_2/ZnO/MnO/K_2O$ (BJ 26, 27, 31) a white, crystalline solid was observed on the catalyst surface after filtration. This solid seemed to decompose during calcination. In one case (BJ 27), the solid was separated from the catalyst by sieving. Analysis of the solid indicated that it contained mainly potassium. Interestingly this catalyst was one of the best in catalytic runs.

For this reason it will be necessary to investigate the impregnation in further detail to determine if this step affects only the palladium content or the alkaline content, as well.

Coprecipitation by Amine Bases

Apart from the influence of the alkali content, the precipitating agent is another parameter that may influence catalyst characteristics. This influence was investigated by using amine bases

instead of alkali hydroxides. In particular, precipitations were performed with ammonia and tetramethylammoniumhydroxide as bases at constant pH levels of 7 and 8, respectively. At high pH levels, dissolution of the metalhydroxides as amine complexes can occur, which will alter the composition. After synthesis the precipitates were washed free from remaining ammonium salts. Subsequently, these catalysts will be impregnated with alkalimetal, being indispensable for higher alcohol synthesis. So far, first characterization results (TG, XRD, BET) resemble those of the alkali precipitated catalysts.

Catalyst Synthesis by Complexation

Apart from coprecipitation, several other catalyst synthesis procedures are being investigated. Complexation is a method that avoids the usual imperfections of coprecipitation methods. It permits the production of amorphous solid compounds with a vitreous structure and a homogeneous composition, without a phase separation from the starting solution. This is achieved by evaporating a solution containing various metallic salts and a complexing agent, generally an -hydroxyacid. Following this route, several catalysts have been prepared. The currently used method will be optimized further.

Catalyst Synthesis by Sol-Gel Methods

Another field that has attracted considerable interest is sol-gel synthesis. Sol-gel processing can offer many advantages for catalyst design:

- purity
- homogeneity
- high thermal stability
- low-temperature processing

The sol-gel process can be described by two simplified chemical reactions: hydrolysis and polycondensation. Both reaction steps can occur in parallel, depending on reaction conditions. Small variations in, for example, precursor concentrations and water/alkoxide ratios can lead to formation of precipitates instead of clear homogeneous sols. Addition of bidentate ligands as acetylacetonate or glycol can prevent precipitation. Acetic acid has been successfully used as well. This method is currently being investigated for the synthesis of ZrO_2/ZnO/MnO and TiO_2/ZnO/MnO catalysts using zirconium and titanium alkoxides as precursors. Specific characterization data will be given in the next report.

Further Developments

The crystalline zinc-manganese phases in the ZrO_2/ZnO/MnO catalysts observed in XRD-spectra could play an important role in the activity and selectivity of these systems. To test this hypothesis, a set of catalysts based on the system M_xO_y/ZnO/MnO is being prepared, where zirconia has been exchanged against titanium, lanthanum or ceria. Several synthesis routes are being examined and will be followed by impregnation with alkali metals.

Appendix

Figure 3.3.1.2. Adsorption Isotherm of Catalyst BJ27

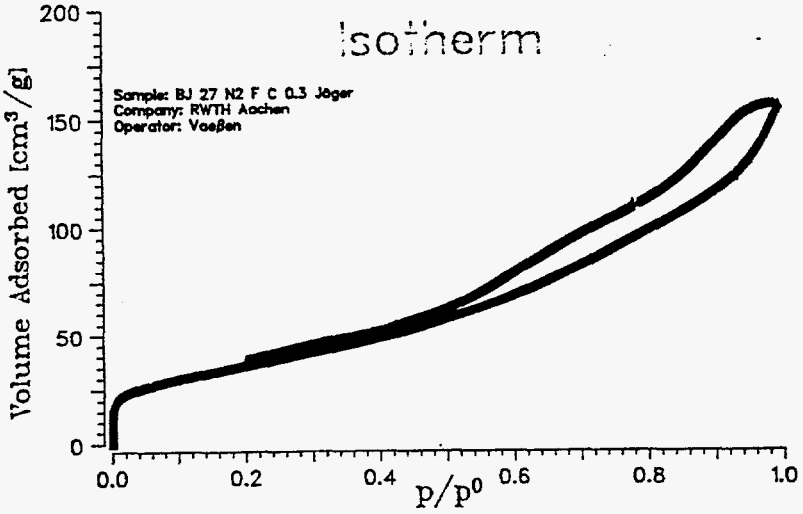

Figure 3.3.1.3. Pore Size Distribution of Catalyst BJ27

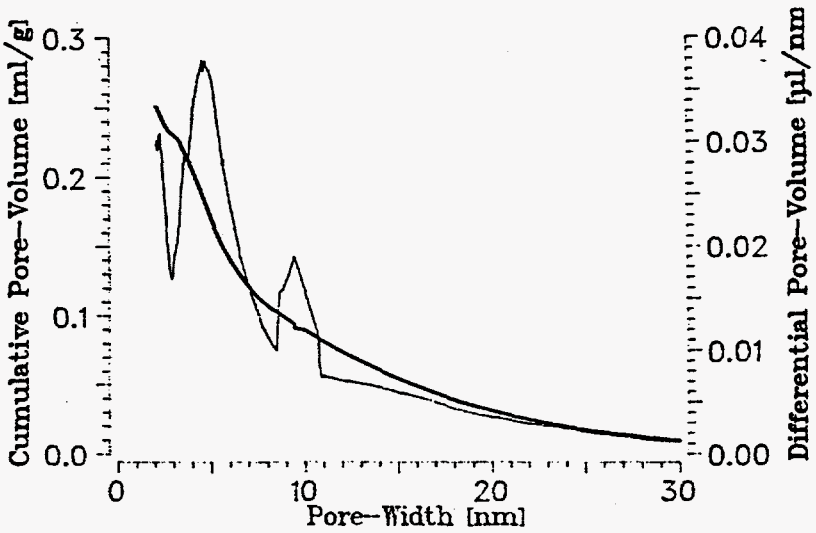

Figure 3.3.1.4. XRD Scan of Catalyst BJ27

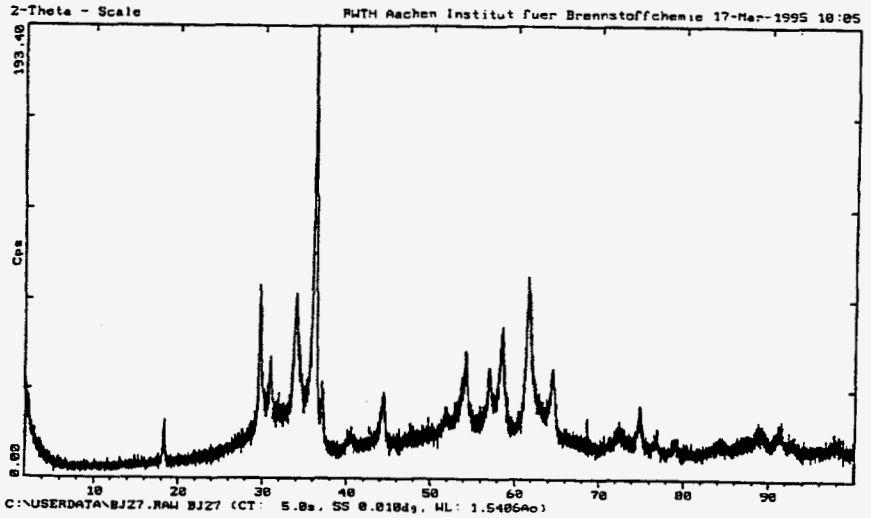

Figure 3.3.1.5. DSC/TG of Catalyst BJ2700

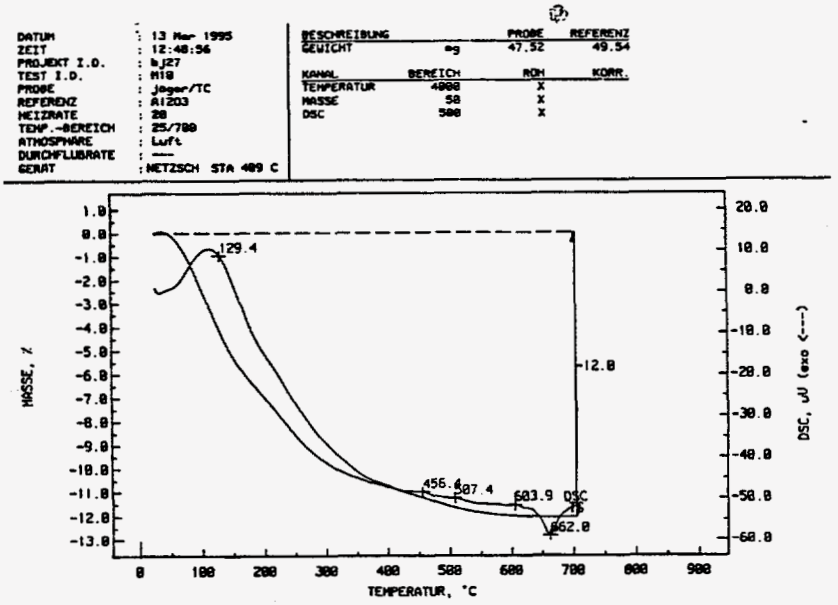

3.3.2 Oxygenates via Synthesis Gas (Lehigh University)

Introduction

During the previous quarter, it was shown that the $Cs/Cu/ZnO/Cr_2O_3$ catalyst was an active alcohol synthesis catalyst at the severe reaction temperature of 340°C, producing 45 g isobutanol/kg cat/hr and 138 g methanol/kg cat/hr. However, some deactivation toward higher alcohols occurred over a period of ≈250 hr. At the same time, the productivity and selectivity toward methanol increased. This quarter, research with this catalyst has focused on (i) the stability of the catalyst at the high reaction temperature of 340°C in $H_2/CO = 0.45$ synthesis gas and (ii) the effect of contact time and pressure on the productivity of the alcohol from $H_2/CO = 0.75$ synthesis gas at 325°C.

New Processes for Mixed Alcohols and Other Oxygenates

I. Overall 2QFY95 Objectives

(i) To continue studies of increasing the surface area and catalytic activity of $Cs/Cu/ZnO/Cr_2O_3$ catalysts for higher alcohol synthesis from H_2/CO synthesis gas

(ii) To prepare and test high surface area Cu/ZrO_2 catalysts that are candidates for the synthesis of C_1-C_5 alcohols, in particular branched products such as isobutanol, and

(iii) To make substantial progress in establishing the accessibility, number, and type (Lewis or Bronsted) and strength of the active surface acid sites by volumetric and HR-XPS analyses after pyridine adsorption on the sulfated zirconia catalyst that is highly active for the selective dehydration of isobutanol to isobutene from methanol/isobutanol reactant mixtures.

Results and Discussion

The preparation, characterization, and testing of catalysts this quarter has centered on oxide catalysts for alcohol synthesis from H_2/CO synthesis gas mixtures. The particular catalysts studied are based on $Cu/ZnO/Cr_2O_3$ and Cu/ZrO_2, and an introduction to the former catalyst, with and without the presence of CsOOCH dopant, was provided in the previous quarterly report.

The preparation of the $Cu/ZnO/Cr_2O_3$ catalyst was described in the previous report, and it was doped with an aqueous CsOOCH solution under a N_2 atmosphere to yield a 3 mol% $Cs/Cu/ZnO/Cr_2O_3$ catalyst. A portion of this catalyst was previously tested in the high temperature range of 310-340°C as a function of the temperature and H_2/CO molar ratio in the reactant mixture. During the present quarter, additional studies have been carried out at 325 and 340°C.

The 3 mol% $Cs/Cu/ZnO/Cr_2O_3$ catalyst has been tested at the severe reaction temperature of 340°C as part of any accelerated stability test. The purpose of the experiment was to follow the

catalyst activity (and in particular the methanol/higher alcohol selectivity) during a long term test and to improve the understanding of deactivation features that affect the ternary catalyst at high temperature. In order to minimize the contribution of the formation of iron carbonyls upstream and deposition of iron onto the catalyst leading to the deactivation of the catalyst, special precautions were taken, and these included larger traps than the previous ones used, fresh activated charcoal and molecular sieve adsorbant materials was installed to purify the CO stream, and a water-cooling circuit was adopted to keep the reactant gas feed zone upstream from the copper-lined reactor in the temperature range of 40-70°C. In absence of a coolant, this zone (by conduction) reached 100-150°C when the reactor temperature was set to 340°C, thus favoring the formation of $Fe(CO)_5$. As usual, a copper-lined reactor was employed.

The catalyst stability experiment was carried out over a period of nearly 400 hr under the following higher alcohol synthesis conditions: GHSV = 5300 l/kg cat/hr, $H_2/CO = 0.45$, T = 340 °C, and P = 7.6 MPa. The trends of methanol and isobutanol productivity are plotted *vs* time of reaction in Figure 3.3.2.1. During the first 50 hr of reaction, a stable behavior of the catalyst was gradually reached. However, the overall activity of the catalyst was lower than expected on the basis of previous experiments. This was probably due to an incomplete degree of reduction of the catalyst. In fact, by gradually removing the CO reactant flow and maintaining the H_2 reactant flow for ≈10 hr (Event I in the figure), a full activity of the catalyst was subsequentely recovered with production of about 140 g/kg cat/hr of methanol and of 43.5 g/kg cat/hr of isobutanol (CO conversion was 14%).

During the following 300 hr of testing, a gradual loss of the catalyst activity toward higher alcohol synthesis, isobutanol as shown in Figure 3.3.2.1, was observed. As expected, the decreasing trend of CO conversion (equal to 8.5% at the end of the experiment) resulted in a gradually increasing formation rate of methanol, thermodynamically constrained to the gas phase composition. As shown in Figure 3.3.2.1, the catalyst activity trend was not drastically decreasing, but it was asymptotic with values of 170 g/kg cat/hr for the productivity of methanol and 22 g/kg cat/hr for the productivity of isobutanol, which was almost stable during the last 200 hr of reaction. Periodic increments of hydrogen partial pressure (in Figure 3.3.2.1, this is indicated as Events II, III, IV, and V where the CO flow was decreased for 3-8 hr to produce a H_2/CO ratio ≈ 5) yielded a temporary benefit to the catalytic activity, e.g. increments of 10-20% in isobutanol productivity accompanied by lowering of methanol productivity were observed after each treatment when testing was continued under the standard operating conditions.

Figure 3.3.2.1. Stability Data for the Cs/Cu/ZnO/Cr_2O_3 Catalyst at 340°C with H_2/CO = 0.45 Synthesis Gas at 7.6 MPa and GHSV = 5300 l/kg cat/hr

At events I-V, the synthesis gas mixture was changed to $H_2/CO \approx 5$ for 3-8 hr by decreasing the CO flow rate (and thus the GHSV).

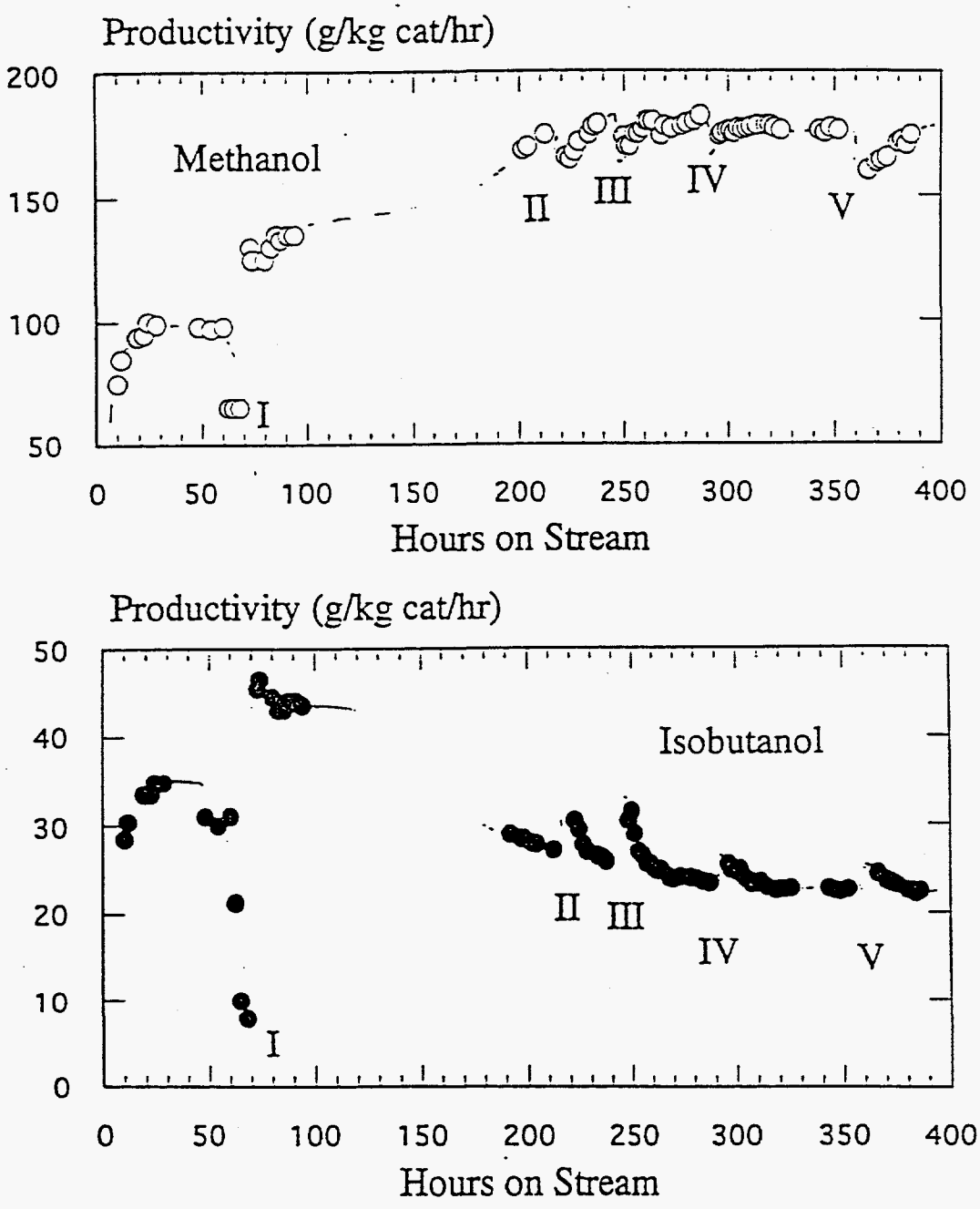

Characterization of this catalyst was carried out before and after testing, and some of the results are summarized here. The catalyst was prepared to give a nominal composition of Cu/Zn/Al = 30/45/25. Elemental analysis yielded the bulk metal ratio for the tested catalyst of 31.0/45.3/23.7. After Cs-doping and calcination at 350°C, the BET surface area was 86 m^2/g. The same surface area was obtained for the tested catalyst. The X-ray powder diffraction (XRD) pattern of the calcined sample showed that it was very poorly crystalline, as shown in Figure 3.3.2.2, where the broad peak at $2\theta \approx 42.5°$ corresponds to CuO. The XRD pattern for the tested catalyst showed the presence of more crystalline ZnO (but still small crystallite size) and metal Cu with a crystallite size ≤100 A, as indicated in Figure 3.3.2.2.

Even with the severe reaction temperature utilized in this experiment, the catalytic testing and characterization of this catalyst suggest that:

1) the state of reduction of the catalyst is critical for its activity and its stability,

2) the loss of activity observed at high temperature is in part reversible and recoverable by exposing the catalyst to an excess of hydrogen,

3) as a consequence of the H_2-rich treatments leading to higher activity, Cu° sintering, which is an irreversible process, cannot be the dominant or at least unique cause of the observed deactivation, and

4) the benefical effect of high H_2/CO feed ratios could be related to the catalyst state of reduction (perhaps not complete under the conditions employed nor stable for low values of hydrogen partial pressure) and/or to the presence of high molecular weight components (waxes) adsorbed on the catalyst surface and subsequent removed by H_2 (although the tested catalyst still exhibited a high surface area).

Figure 3.3.2.2. X-Ray Powder Diffraction Patterns of the Cs/Cu/ZnO/Cr_2O_3 Catalyst After Calcination and After Catalytic Testing

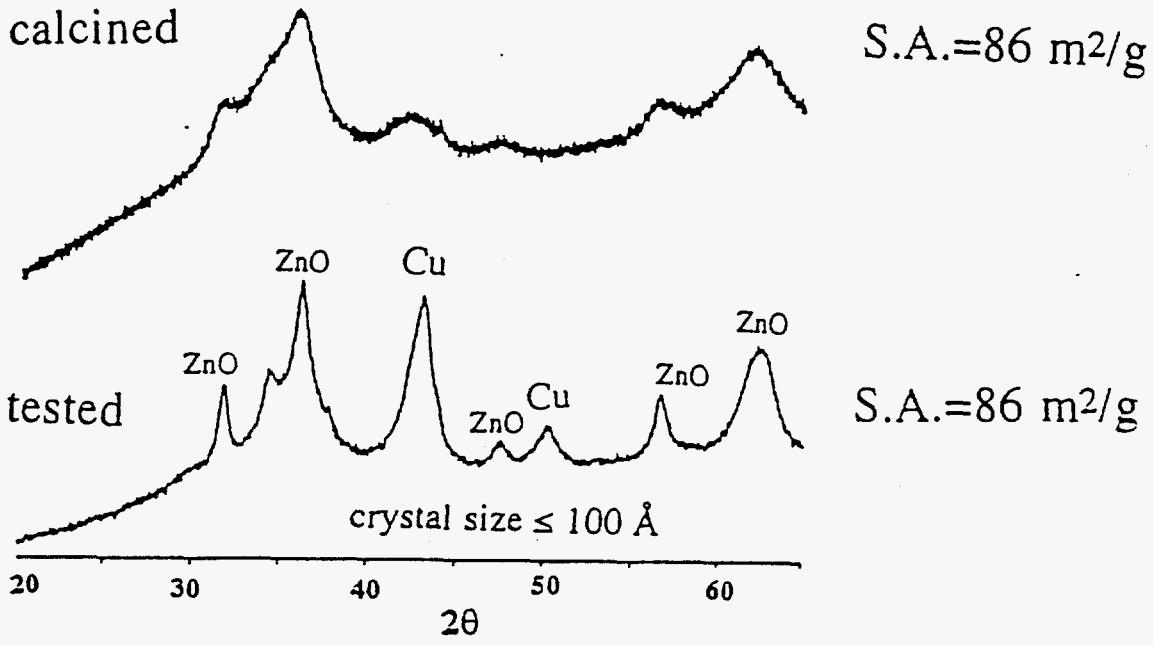

Further investigation of the performance of the Cs-promoted ternary Cu/ZnO/Cr_2O_3 catalyst was carried with respect to the effects that residence time and total pressure of the reactants exert on the production and distribution of methanol and higher alcohols. Kinetic runs have been performed at different values of gas hourly space velocity (GHSV) in the range of 3,300-18,300 l/kg cat/hr for two values of total pressure (7.6 and 6.5 MPa). The experiments were performed at the reaction temperature of 325°C and with a H_2/CO molar ratio equal to 0.75, which has already been reported to be optimal with respect to higher oxygenates.

It was observed that as the residence time increased, the productivity of methanol and linear alcohols decreased. However, as shown in Figure 3.3.2.3, this effect was less significant with the 2-methyl-1-propanol (isobutanol) product, especially at the lower pressure of 6.5 MPa. From Figure 3.3.2.3, it can be observed that:

- High space velocity values (short contact times) significantly favor the productivity of methanol, which reached over 1000 g/kg cat/hr.
- At the higher pressure, the productivity of all the higher oxygenates increases with increasing gas space velocity up to a maximum value beyond which further increments of space velocity make the residence time the limiting factor in the formation of higher alcohols (secondary products). An optimal production of oxygenates has been observed for GHSV = 12,000 l/kg

cat/hr, where the overall productivity of ethanol, propanol, and isobutanol approaches 250 g/kg cat/hr.

- At the lower pressure, the rate of formation of the linear and branched alcohols became slower at short contact times. On the contrary, at longer contact times (low space velocities), higher alcohol synthesis seems to be enhanced by lower reaction pressure. This comparison suggests that the formation of C_2+ oxygenates tends to slow down with increasing contact times at higher pressure, perhaps due to the inhibiting effect of adsorption phenomena that are expected to be more significant at high pressure. It is finally noted that at lower pressure, methanol formation is significantly reduced, and this provides high selectivities to higher oxygenates at longer residence times.

Figure 3.3.2.3. Effects of the Contact Time and the Total Pressure of the $H_2/CO = 0.75$ Synthesis Gas Reactant on the Productivities of the C_1-C_6 Alcohols at 325°C
Indicated are the linear and 2-methyl branched alcohols.

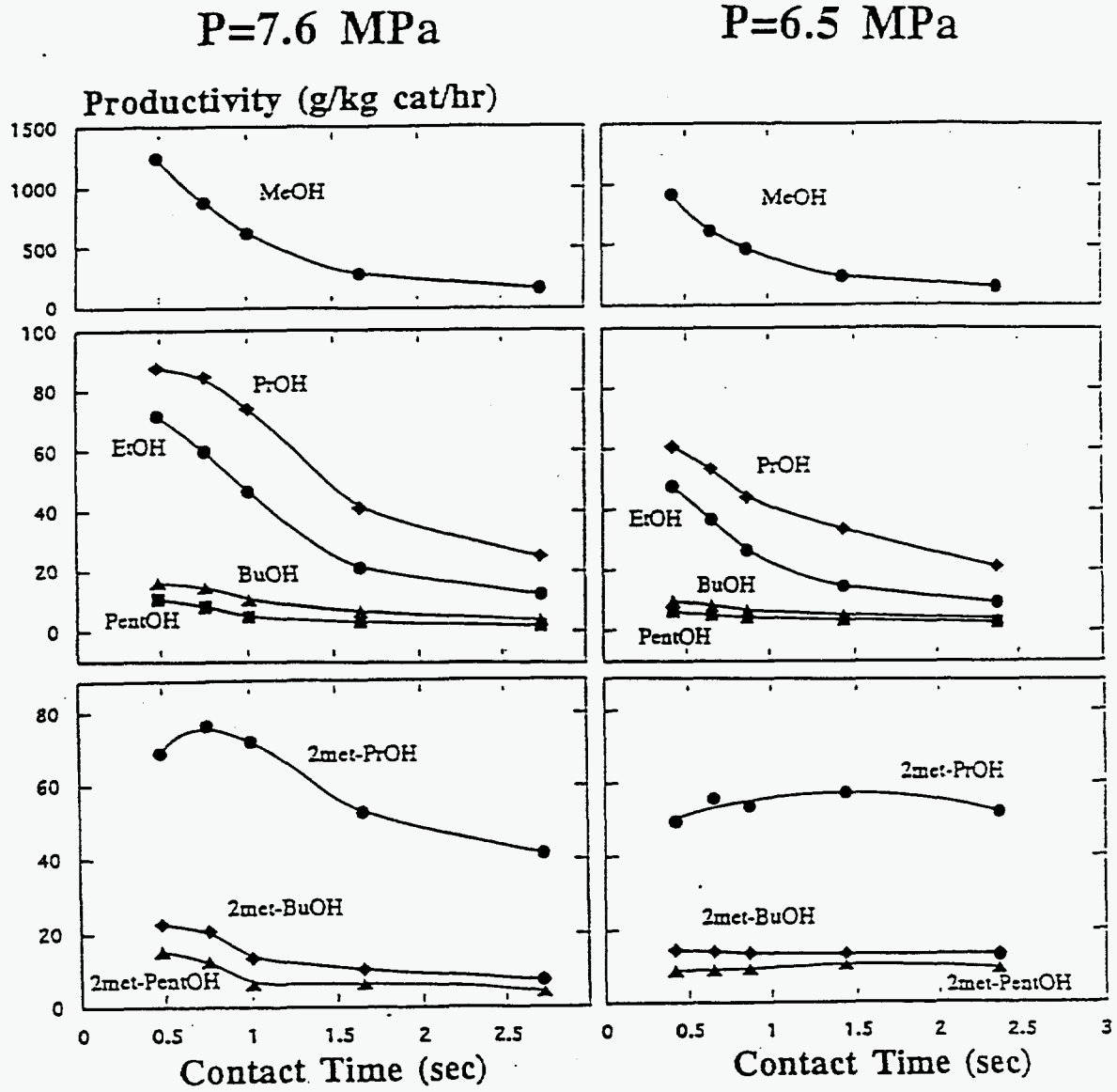

Cu/ZrO_2 Catalysts

Zirconia-based catalysts are being investigated for their potential as alcohol synthesis catalysts. In particular, a series of CuO/ZrO_2 catalysts having different Cu/Zr molar ratios have been prepared and initial characterization studies have been carried out with the precursors and the calcined oxides before catalytic testing is initiated.

The catalysts were prepared by aqueous coprecipatation at constant pH and temperature. A weighed quantity of $Cu(NO_3)_2 \cdot 2.5H_2O$ was dissolved in distilled water to make a 0.5 M solution. Similarly, a 0.5 M $ZrO(NO_3)_2 \cdot 6H_2O$ solution was prepared. These two solutions were mixed to give the desired Cu and Zr molar ratios of 10/90 and 30/70 in the final products. A basic buffer solution, used to control the pH, was prepared by mixing together 2 M sodium hydroxide and 2 M sodium acetate solutions.

Aqueous solutions of $ZrO(NO_3)_2 \cdot 6H_2O$ and $Cu(NO_3)_2 \cdot 2.5H_2O$ and of the buffer solution were poured into two separate dropping funnels. The reagents were added dropwise into a Pyrex flask containing 250 ml deionized water at 90°C that was vigorously stirred. The addition of these two solutions was adjusted to maintain the pH at about 7. Approximately 30 min was taken to complete the precipitation, and the resultant solid was allowed to digest for 45 min. The precipitate was then filtered and thoroughly washed with ≈4000 ml of warm deionized water. The color of the residue was deep blue. The dense mass was then dried in ambient atmosphere over a period of 48 hr. A significant amount of volume shrinkage occurred due to the loss of water and the color changed to dark blue. During filtration and washing, the wash water was not colored, indicating no loss of copper in this process. The precursors were crushed into pieces and kept at 110°C for another 24 hr to complete drying.

Separate samples of both of the precursors were calcined at 350°C, 400°C, and 500°C for 3 hr at each temperature. Surface area measurements (BET using N_2) were carried after calcination at the aforesaid temperatures. X-Ray powder diffraction patterns were obtained at each step to investigate the structural aspect of the material.

Significant surface areas were observed for the CuO/ZrO_2 = 10/90 mol% catalyst, as shown in Table 3.3.2.1. The surface areas for the 30/70 catalyst were lower but still appreciable. The dried precursors were X-ray amorphous, and the precursors calcined at 350°C and 400°C did not show the presence of crystalline components, as illustrated by Figure 3.3.2.4. However, precursors calcined at 500°C showed the presence of tetragonal ZrO_2, as indicated in Table 3.3.2.1 and in Figure 3.3.2.5. There was no evidence of crystalline CuO even after the precursors were calcined at 500°C. Dried precursors calcined at all these temperatures exhibited weight losses of about 16-18%.

Table 3.3.2.1. Surface Areas and X-ray Powder Diffraction Information for the CuO/ZrO_2 Materials After Calcination at 350, 400, and 500°C.

CuO/ZrO_2 Sample	Calcination Temperature	Surface area (m^2/g)	XRD Crystallinity
(10/90)	350°C	149	Amorphous
(10/90)	400°C	112	Amorphous
(10/90)	500°C	63	Tetragonal ZrO_2 CuO not detected
(30/70)	350°C	78	Amorphous
(30/70)	400°C	73	Amorphous
(30/70)	500°C	25	Tetragonal ZrO_2 CuO not detected

Overall 3QFY95 Objectives

Future plans for Task 3.3.2 will focus on the following areas:

(i) To continue studies of increasing the conversion of H_2/CO to higher alcohols by promotion of the $C_1 \rightarrow C_2$ carbon chain growth step over Cs-promoted $Cu/ZnO/Cr_2O_3$ and MoS_2 catalysts,

(ii) To enhance the $C_2 \rightarrow C_3 \rightarrow C_4$ carbon chain growth steps over $Cs/Cu/ZnO/Cr_2O_3$ catalysts, and

iii) To prepare and test high surface area Cu/ZrO_2 catalysts, both Cs-doped and undoped, that are candidates for the synthesis of C_1-C_5 alcohols, in particular branched products such as isobutanol.

3.3.3 Study of Catalyst Preparation, Calcination, and Alkali Doping for Isobutanol Synthesis (University of Delaware)

Introduction

In this quarter, our study focused on the preparation, reaction testing, and characterization of the catalysts. By varying the factors, such as the basic precipitant (KOH instead of K_2CO_3), the calcination atmosphere (under nitrogen instead of air), and various dopant alkali metals, we were able to test for the sensitivity of isobutanol synthesis to these effects. The goal of these experiments is to improve isobutanol productivity from CO hydrogenation on our previously developed catalysts. From the following report, it is clearly seen that the KOH precipitation and nitrogen calcination significantly enhance the total alcohol productivity, and most importantly, the isobutanol selectivity. In addition, KOH precipitation leads to a suppression of n-propanol production, which is important since n-propanol is the major higher alcohol other than isobutanol produced on our catalysts. X-ray diffraction from the bulk structure of the new catalysts indicates no structurally significant feature that sets these materials apart from the previous

Figure 3.3.2.4. X-Ray Powder Diffraction Pattern of the CuO/ZrO_2 = 10/90 mol% Catalyst After Calcination at 350°C in Air
The peak at ≈44° is attributable to the sample holder.

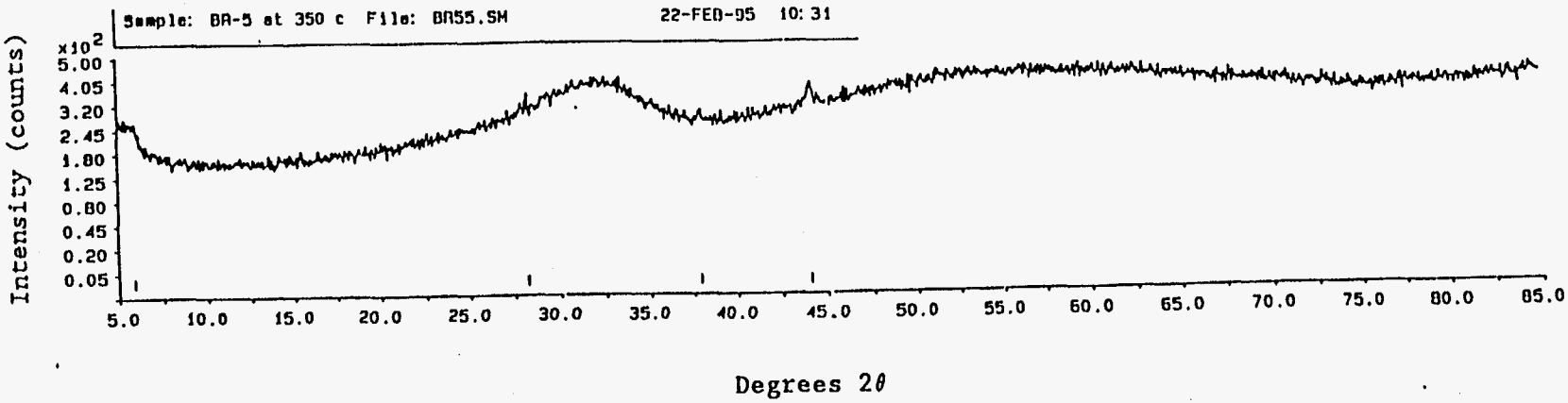

Figure 3.3.2.5. X-Ray Powder Diffraction Pattern of the CuO/ZrO_2 = 10/90 mol% Catalyst After Calcination at 500°C in Air

The peak at ≈44° is attributable to the sample holder.

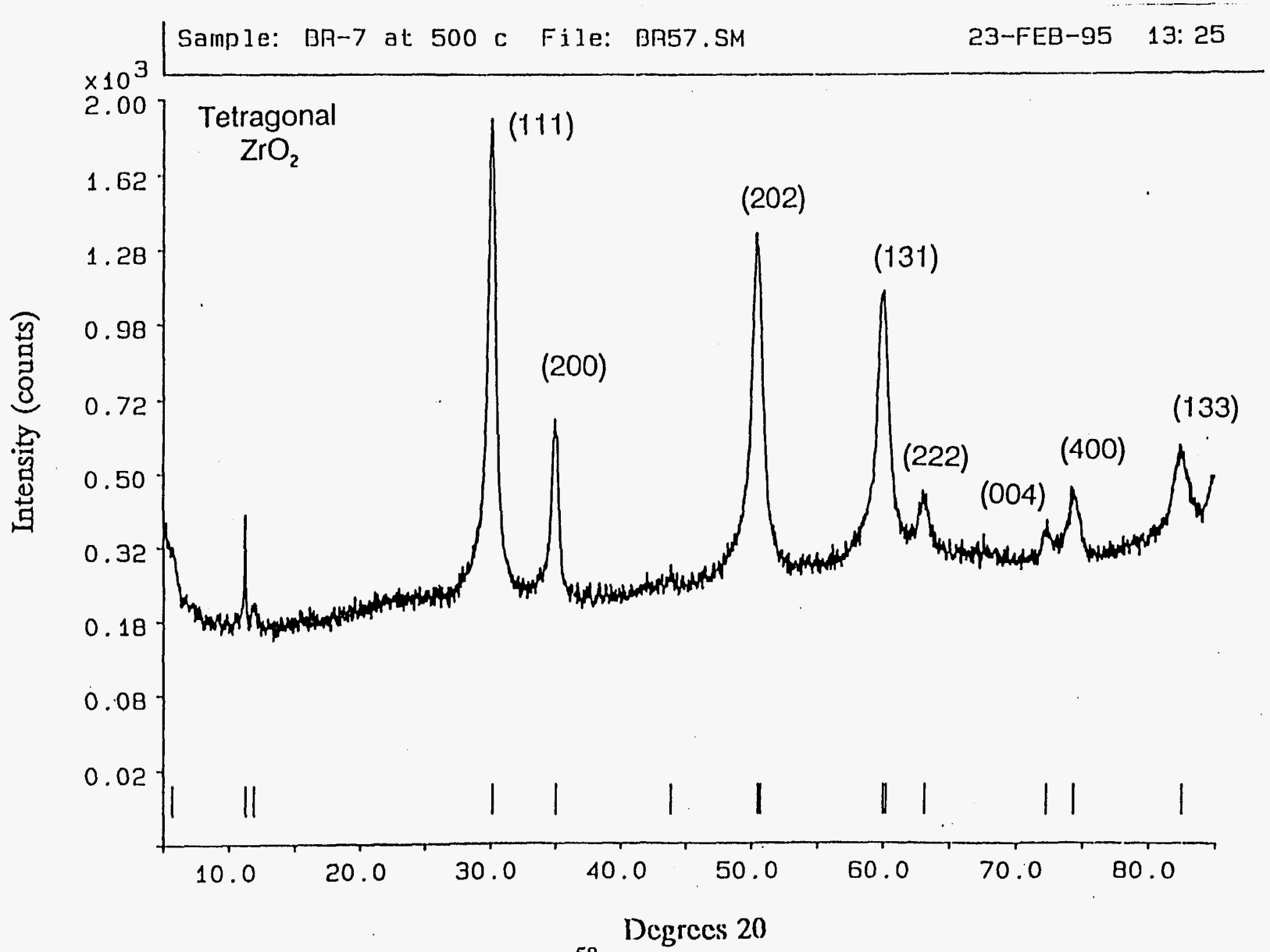

catalysts. This strongly suggests that the catalyst performance is enhanced by a tuning of the surface sites in a manner that is not diagnosable in the bulk.

Experimental

The comparison of nitrogen calcination and air calcination of the catalysts was performed on catalysts with compositions corresponding to F6K and F7K (Table 3.3.3.1), which were calcined in flowing air. The corresponding catalysts, calcined under flowing nitrogen, are coded as F6NK and F7NK. The catalysts were prepared by dropping the required amounts of metal nitrate solution into K_2CO_3 (0.2M) basic solution until neutral pH was reached (at precipitation temperature 60°C). The precipitates were washed with deionized water, dried at 130°C (overnight), calcined at 400°C under air or nitrogen flow (3h), pelletized, and sieved. The calcined catalysts were then doped with 4 wt % of K_2CO_3 followed by drying overnight at 130°C. The KOH-precipitated, nitrogen-calcined catalyst reported here is coded as F6KOHN, and it has the same composition as F6K. It was prepared by dropping 2M KOH solution into nitrate solution at 60°C to a final pH of 12. The same process was used for nitrogen calcination as described above.

The reaction testing of the catalysts was carried out at T = 350, 400, 425°C, P = 1000 psi, CO/H_2 = 1, GHSV = 2900/h after 24h reduction of the catalyst with 5% H_2/N_2 at 260°C. The reaction was run for over 20 hours at each temperature. X-ray diffraction patterns of the samples before and after reaction were collected on an XRG-3000 diffractometer with CuKα radiation (45 kV and 40 mA) in the range of 2Θ = 10-90°.

Table 3.3.3.1 Catalyst Compositions and Preparation Methods

Catalysts	Compositions	Preparations
F6K	Mn/Cu = 0.5, Zn/Cu = 0.5, Zr/Cu = 2, CoO = 0.2 wt%, 4 wt% K_2CO_3 doping	Coprecipitation by dropping nitrate solution to K_2CO_3 solution. Final pH = 7, washed, air-calcined
F6NK	Same as above	Same as above except nitrogen calcination
F6KOHN	Same as above except no K_2CO_3 doping	Coprecipitation by dropping KOH solution to nitrate solution. Final pH = 12, nitrogen-calcined
F6KOHNK	Same as above except 4 wt% K_2CO_3 doped	Same as above, K_2CO_3 doped after calcination
F6KOHNLi	Same as F6KOHN but with 4 wt% $LiNO_3$ doping	Same as F6KOHN but with $LiNO_3$ doping
F6KOHNCs	Same as F6KOHN but with 4 wt% $CsNO_3$ doping	Same as F6KOHN but with $CsNO_3$ doping

Results and Discussion

1. Nitrogen Calcination vs. Air Calcination

In order to evaluate the effects of nitrogen and air calcination on the catalytic performance of the previously developed catalysts, we prepared the nitrogen-calcined catalyst, F6NK, for comparison with the air-calcined F6K. The experimental results are listed in Table 3.3.3.2

Table 3.3.3.2 Liquid Product Distributions on the Differently Calcined Catalysts

(@ 425°C, 1000 psi, CO/H_2 = 1, GHSV = 2900/h)

Cat	MeOH	EtOH	iPrOH	nPrOH	2BuOH	iBuOH	nBuOH	Other	Yield
				wt%					g/g/h
F6K	10.6	2.9	6.0	15.4	4.6	18.7	1.5	40.2	9.40E-02
F6NK	7.2	5.2	6.0	23.9	6.2	25.2	2.3	24.0	1.10E-01

The nitrogen-calcined catalyst, F6NK, exhibited improved selectivity toward isobutanol. A significant enhancement of the total higher alcohol selectivity also was observed. Accompanying this effect was the enhancement of n-propanol selectivity. These results indicate that the calcination atmosphere in the catalyst preparation plays a critical role in the performance of catalysts for higher alcohol synthesis. In the strictest sense, calcination is heat treatment of an inorganic solid under flowing air. Our findings indicate that the heat treatment is better done under flowing nitrogen.

The activity, hydrocarbon and carbon dioxide selectivity, and stability of F6K and F6NK are shown by the time on-stream plots in Figures 3.3.3.1 and 3.3.3.2. Both catalysts had relatively stable performance during more than 60 hours of reaction. The nitrogen-calcined catalyst showed better low temperature activity than the air-calcined catalyst (350-400°C). The air-calcined catalyst, on the hand, was slightly more active than the nitrogen-calcined catalyst at 425°C.

The XRD patterns of the catalysts calcined under nitrogen are identical to those for the corresponding catalysts calcined under air (see Figures 3.3.3.3 and 3.3.3.4). Therefore, the improved performance of the catalysts by nitrogen calcination does not arise from detectable changes in the bulk crystal structures of these materials, suggesting that a more subtle surface modification is responsible. The XRD pattern in Figure 3.3.3.4 also shows that metallic copper is the major copper phase while all the other components show up as oxide phases. The level of copper agglomeration is not surprising, but must be limited to enhance activity.

2. KOH Precipitation vs. K_2CO_3 Precipitation

Our investigation of the more subtle effects of preparation variables on catalyst performance reveals that the precipitant has a strong effect. To examine KOH as a basic precipitant, the composition of the catalyst was selected to be that of catalyst F6, which was the best composition for isobutanol production in the previously reported factorially designed sample matrix. In these experiments KOH instead of K_2CO_3 for precipitation, and nitrogen instead of air for calcination were employed.

Nitrogen calcination significantly enhanced isobutanol selectivity and total alcohol productivity, as discussed in the last section. However, n-propanol selectivity was still fairly high for the nitrogen-calcined catalysts (see F6NK in Table 3.3.3.3). With KOH as the basic precipitant, not only was the ease of washing and filtering of the precipitated mixture enhanced, but it also produced catalysts that show significant suppression of n-propanol production while maintaining isobutanol selectivity. Another feature that the KOH precipitated catalysts showed is enhanced

Figure 3.3.3.1. Reaction Performance of F6K (300-425°C, 1000 psi, $CO/H_2 = 1$)

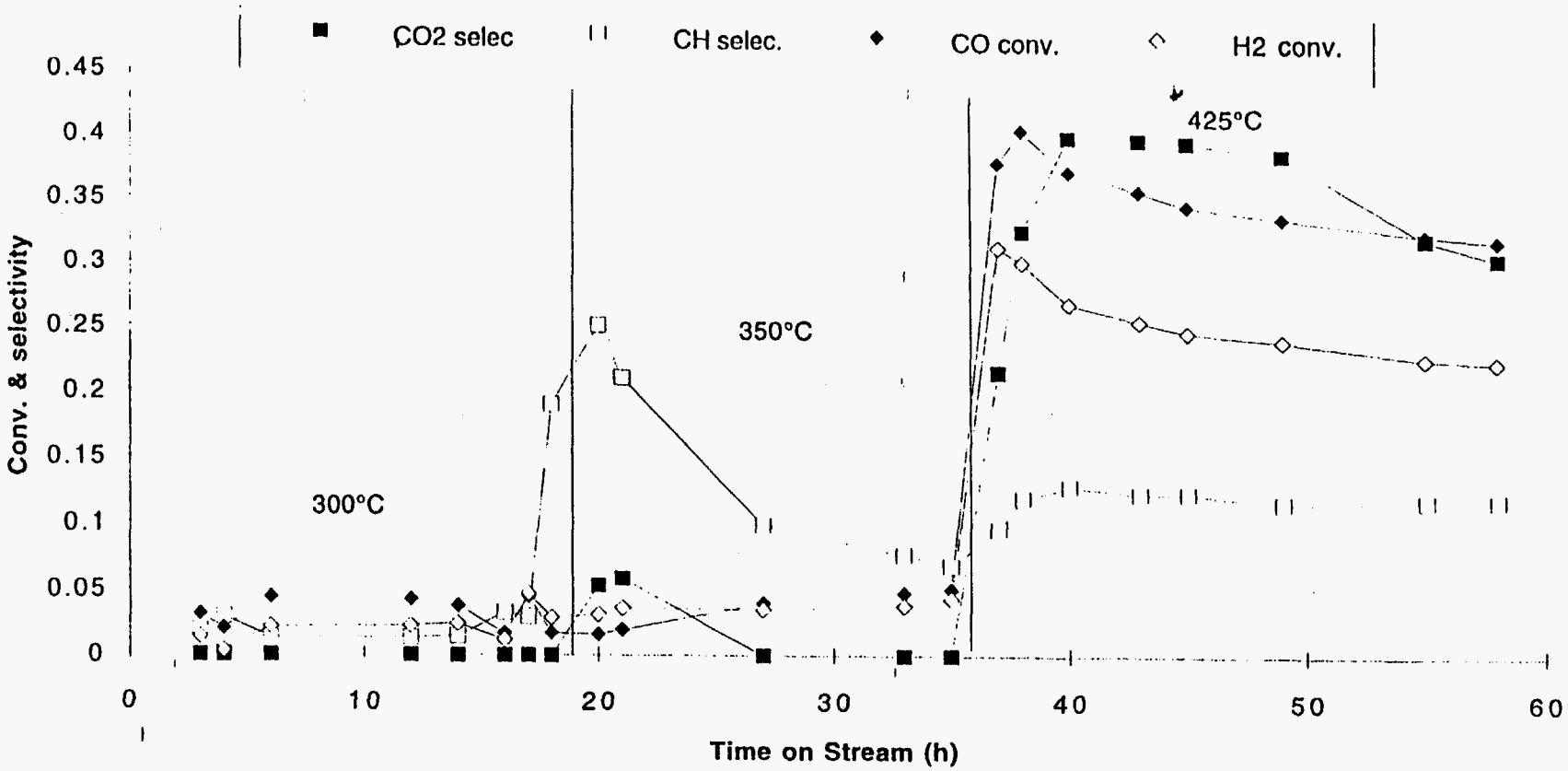

Figure 3.3.3.2. Reaction Performance of F6NK (400-425°C, 1000 psi, $CO/H_2 = 1$)

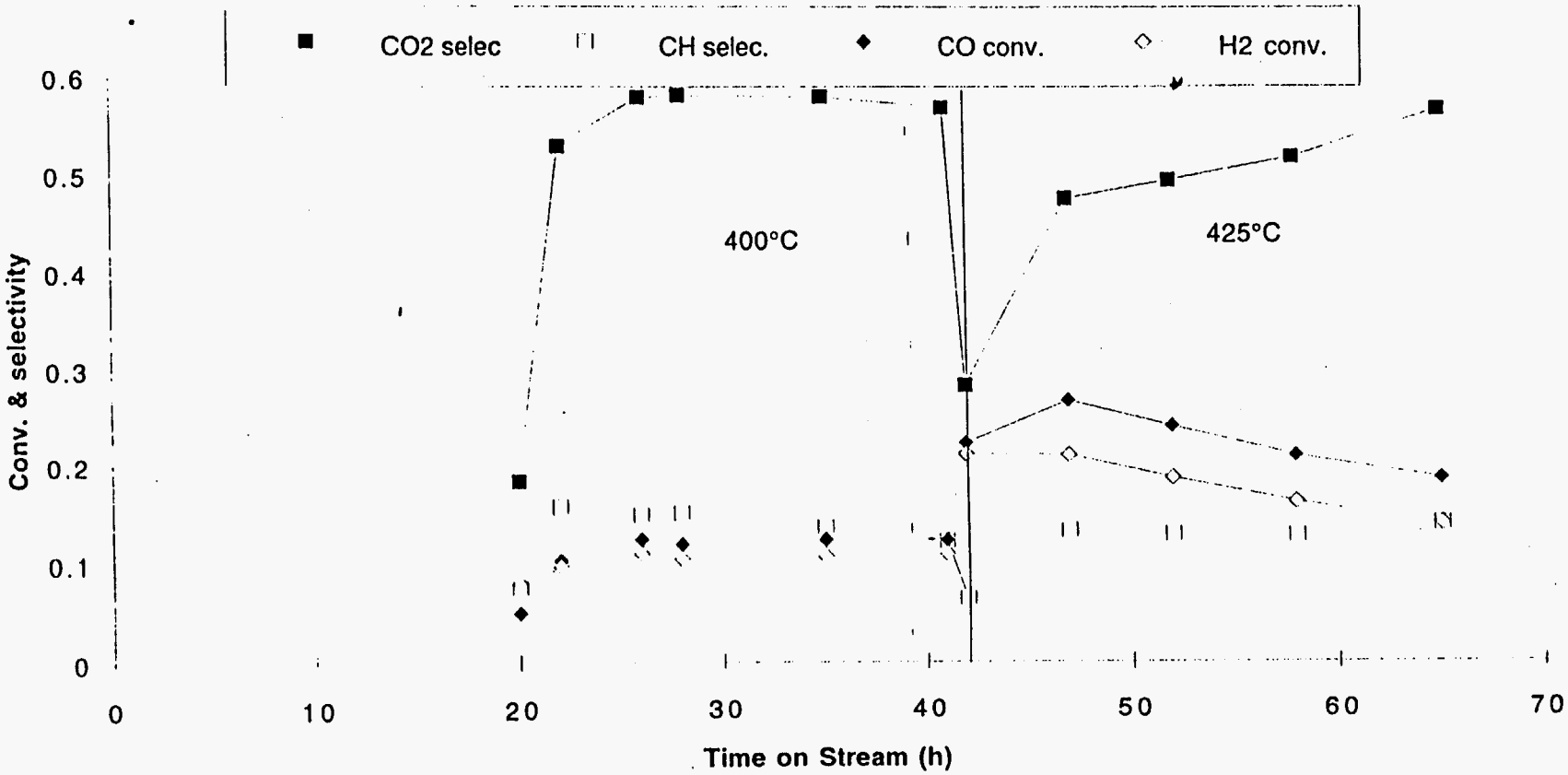

Figure 3.3.3.3. XRD for F6K and F6NK

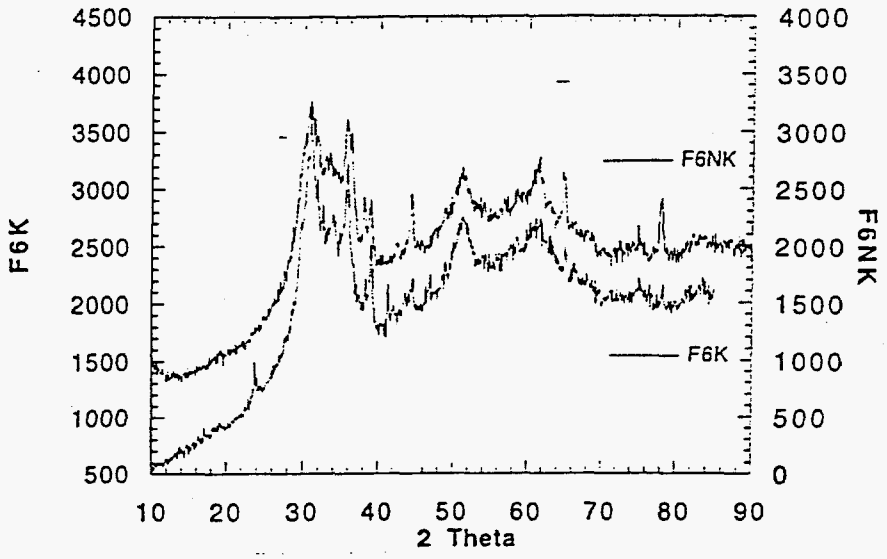

Figure 3.3.3.4. XRD for Used F6K and Used F6NK

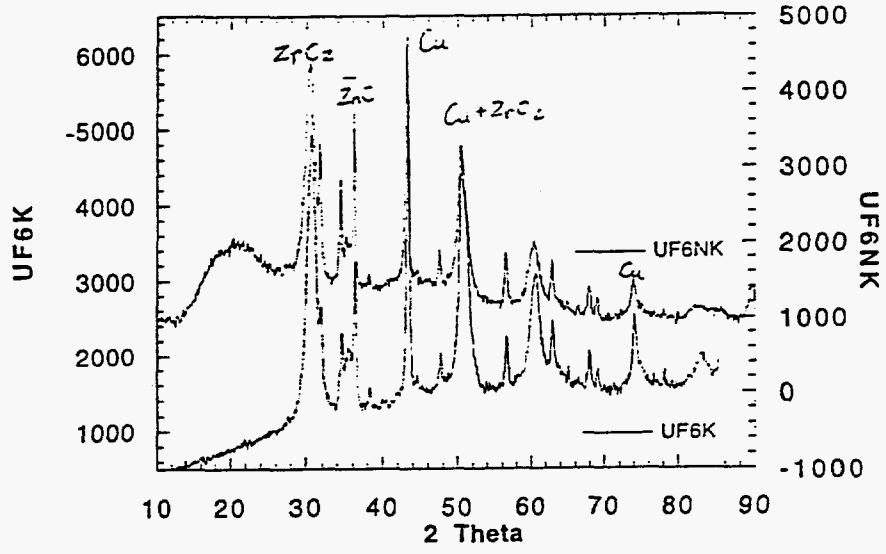

low temperature isobutanol selectivity. For K_2CO_3 precipitated catalysts, for example, F6K and F6NK, the highest isobutanol selectivity is observed at 425°C, the upper temperature limit we applied. But KOH precipitated F6KOHN series of catalysts showed the highest isobutanol selectivity at significantly lower temperature, 400°C. The decreased reaction temperature for reaching the highest isobutanol selectivity is obviously beneficial for suppressing n-propanol selectivity and other by-products. This coupled with other results make it clear that it is possible to optimize isobutanol production through a combination of reaction temperature, catalyst composition, catalyst preparation procedure, and other reaction conditions.

Higher final pH (= 12) in the preparation of F6KOHN in contrast with pH = 7 in the F6NK preparation is another factor that should be taken into account when comparing the performance of F6NK and F6KOHN, because the surface acidity (or basicity), which may depend on the precipitation pH, plays an important role in mixed oxide catalysts. However, this cannot be discussed without a more comprehensive experimental result. This should be one of the subjects to be further studied.

The XRD patterns of the catalyst prepared by KOH precipitation are identical with those for the corresponding catalysts prepared by K_2CO_3 precipitation. The XRD patterns in Figure 3.3.3.5 indicate that bulk structures of the precipitated catalysts after calcination are highly amorphous. As observed for K_2CO_3-precipitated catalysts, the bulk structure of the KOH-precipitated catalyst was transformed into highly crystalline metallic copper and the oxide phases of the other components after reduction and with long time on-stream (see Figure 3.3.3.6). The XRD data do not provide a clue to the reason for the enhanced performance of the KOH-precipitated catalysts, indicating that a more subtle surface-modification of the catalyst is responsible for the selectivity rise.

3. Effects of Alkali Doping for KOH Precipitated Catalysts

When we made the comparison between the K_2CO_3-precipitated catalyst and the KOH-precipitated catalysts, we were comparing F6NK with the whole series of alkali-doped catalysts (F6KOHNK, F6KOHNLi, F6KOHNCs). In fact, the reaction results on F6KOHNK are an exception in the series since the reaction on it was run at low GHSV (half of the standard run due to leaking at reactor inlet). We expect that the liquid product distribution on F6KOHNK would be similar to that for the Li and Cs doped catalysts if it had been run under normal conditions. We did not repeat the reaction on F6KOHNK because a more consistent conclusion was obtained from comparison of undoped catalyst F6KOHN and the alkali doped catalysts.

F6KOHN, a catalyst left undoped with no alkali metal component, has shown excellent isobutanol selectivity and suppressed n-propanol selectivity (see Table 3.3.3.3). These results suggest that the excess alkali doping does not play a role in improving the isobutanol selectivity and higher alcohol productivity of the previously discussed catalysts. This result is surprising since it is not in agreement with expectation based on the commonly accepted idea that alkali promotion enhances higher alcohol synthesis. A possible reason for the observed result might be that potassium residue from the original KOH-precipitation process provides adequate promotion. This issue will be examined by submitting the catalysts to elemental analysis and other tests for the preserved effect of potassium. With regard to liquid productivity, the undoped

Figure 3.3.3.5. XRD for F6NK and F6KOHN

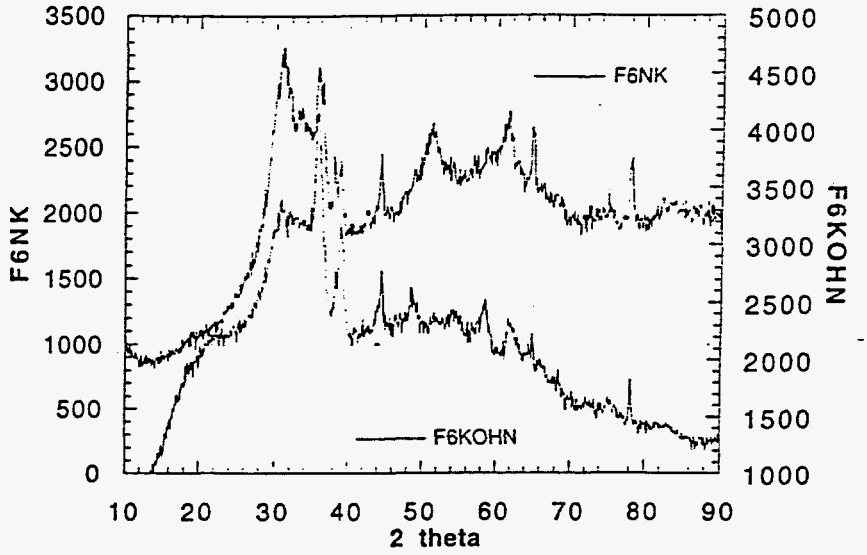

Figure 3.3.3.6. XRD for Used F6NK and Used F6KOHN

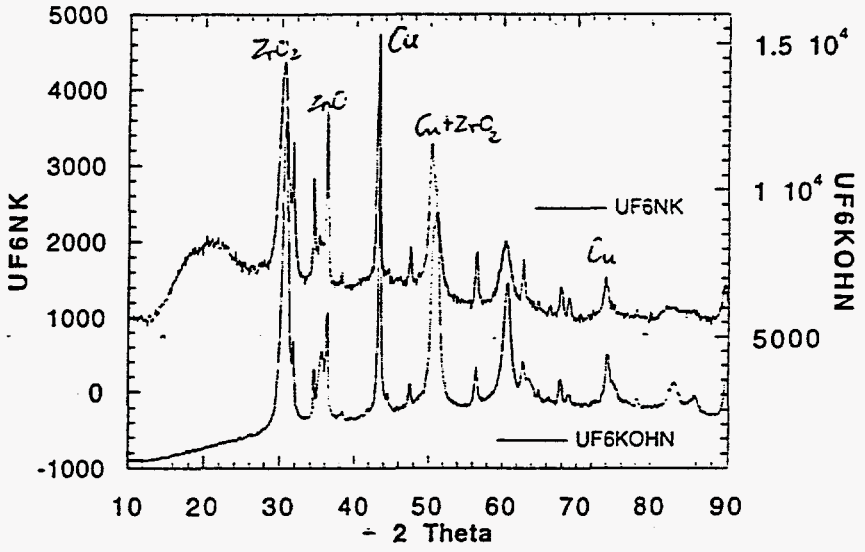

catalyst, F6KOHN, has shown the same or even higher (at 400°C or lower temperature) liquid yield compared with Li-, Cs-, or K-doped catalysts. The lower activity might be expected for excess alkali-doped catalysts, if the alkali components cover or block some of the active sites on the catalyst's surface. This too will be investigated.

Time on-stream performance of the F6KOHN series of catalysts is shown in Figures 3.3.3.7 through 3.3.3.10. Generally, this group of catalysts shows relatively stable activity during 60 hours of reaction at 350 to 425°C. Relatively low hydrocarbon selectivity and high carbon dioxide selectivity were observed on all of these catalysts.

The reaction test of F6KOHNLi at 400°C after 20 hours on-stream at 425°C showed that not only was the catalyst significantly deactivated, but the original selectivity pattern observed at 400°C could not be recovered completely (see Table 3.3.3.3 and Figure 3.3.3.8). This indicates that the active sites for isobutanol production may not be stable at higher temperatures, whereas those leading to n-propanol may be increasing. This result, along with the effect of nitrogen calcination and KOH precipitation, further substantiates the role that subtle surface modifications may play in these catalysts.

Table 3.3.3.3 - Liquid Product Distribution on Different Catalysts (wt%)
(@ 1000 psi, CO/H_2 = 1, GHSV = 2900/h)

Cat/Temp.	MeOH	EtOH	iPrOH	nPrOH	2BuOH	iBuOH	Other	Yield (g/g/h)
F6NK								
350	65.2	11.3	2.3	17.2	0.5	5.5	1.9	0.003
400	21.7	12.2	5.2	28.9	3.3	17.5	11.3	0.070
425	7.2	5.2	6.0	23.9	6.2	25.2	26.3	0.110
F6KOHNK								
350	45.5	3.8	0.0	5.9	0.0	15.1	29.1	0.028
400	17.4	6.2	0.0	12.5	0.0	13.8	50.1	0.083
425	10.4	3.8	1.0	13.3	0.9	10.1	60.5	0.098
F6KOHNCs								
350	57.4	1.8	0.0	2.8	0.0	15.2	22.9	0.047
400	23.4	3.8	0.0	6.2	0.0	23.6	43.0	0.074
425	12..8	6.6	0.0	14.5	0.0	13.1	51.3	0.105
F6KOHNLi								
350	61.4	1.8	0.0	2.4	0.0	17.7	16.7	0.050
400	25.3	4.5	0.0	5.9	0.0	22.9	41.4	0.078
425	13.6	5.5	0.0	14.3	0.0	13.0	53.6	0.105
400 after 425	26.3	5.7	0.0	16.2	0.0	12.9	38.9	0.050
F6KOHN								
350	69.2	0.0	0.0	1.1	0.0	14.8	14.3	0.060
400	27.3	0.0	0.0	2.0	0.0	24.0	46.7	0.083
425	13.3	2.9	1.4	5.6	0.0	19.3	57.4	0.086

Figure 3.3.3.7. Reaction Performance of F6KOHN (350-425°C, 1000 psi, $CO/H_2 = 1$)

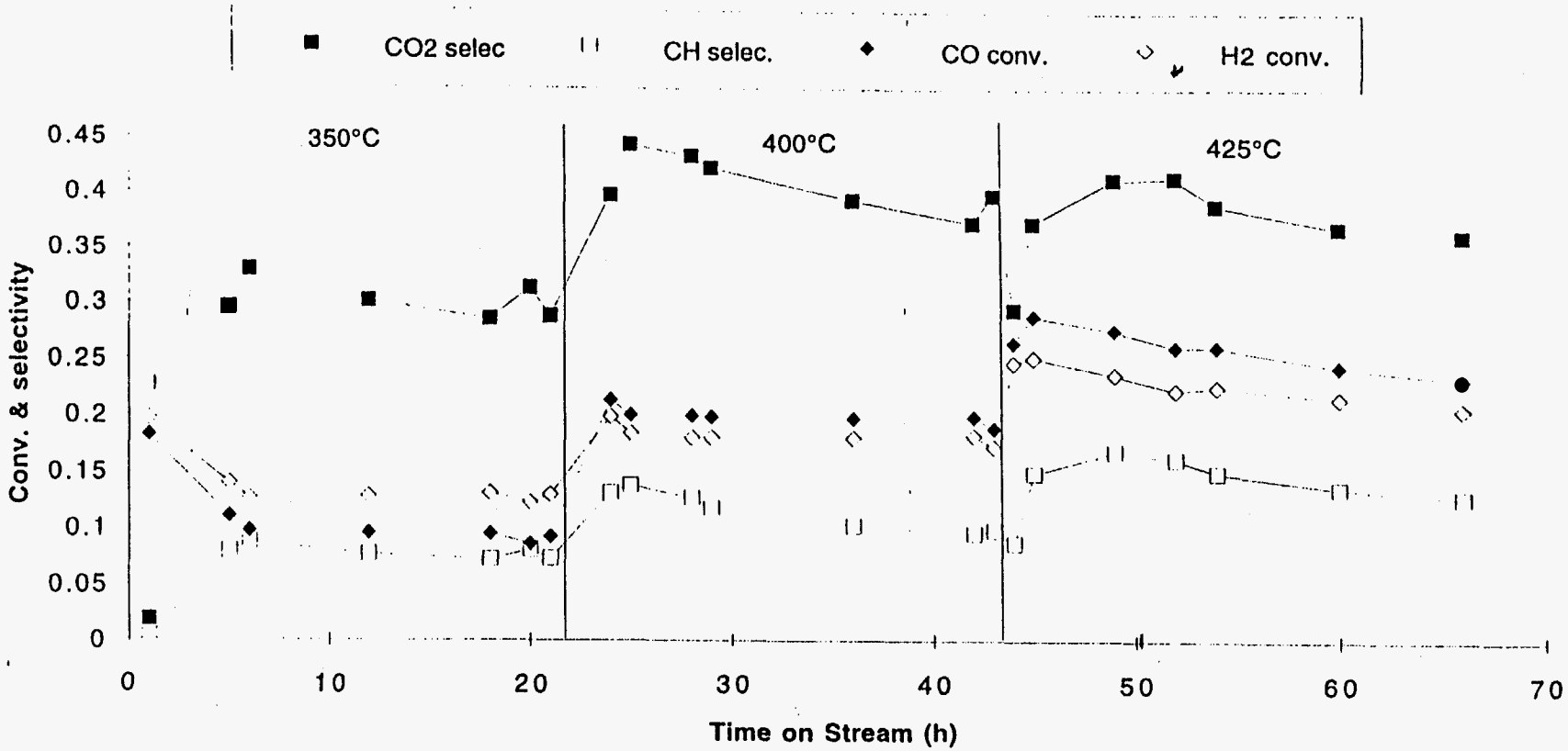

Figure 3.3.3.8. Reaction Performance of F6KOHNLi (350-425°C, 1000 psi, $CO/H_2 = 1$)

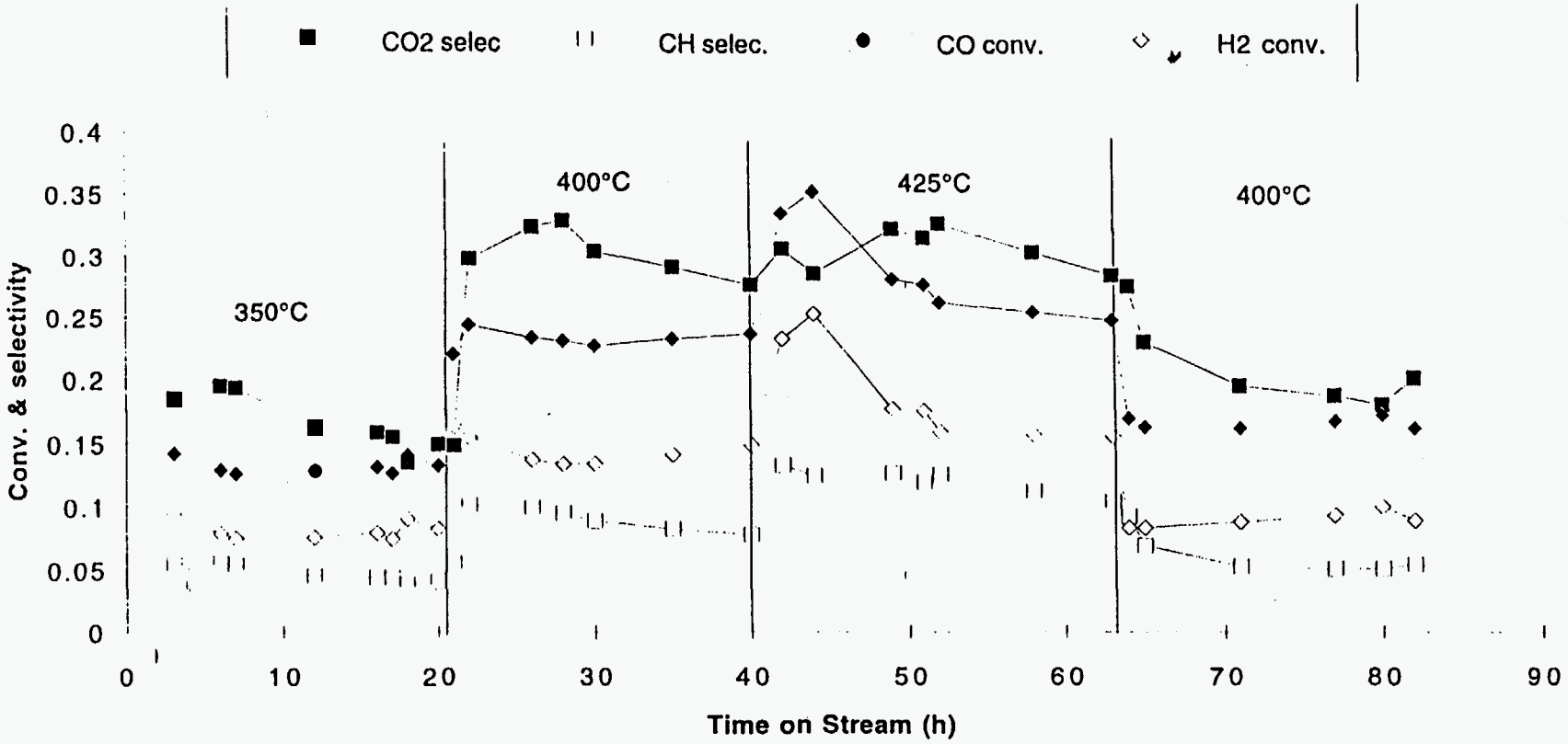

Figure 3.3.3.9. Reaction Performance of F6KOHNK (350-425°C, 1000 psi, $CO/H_2 = 1$)

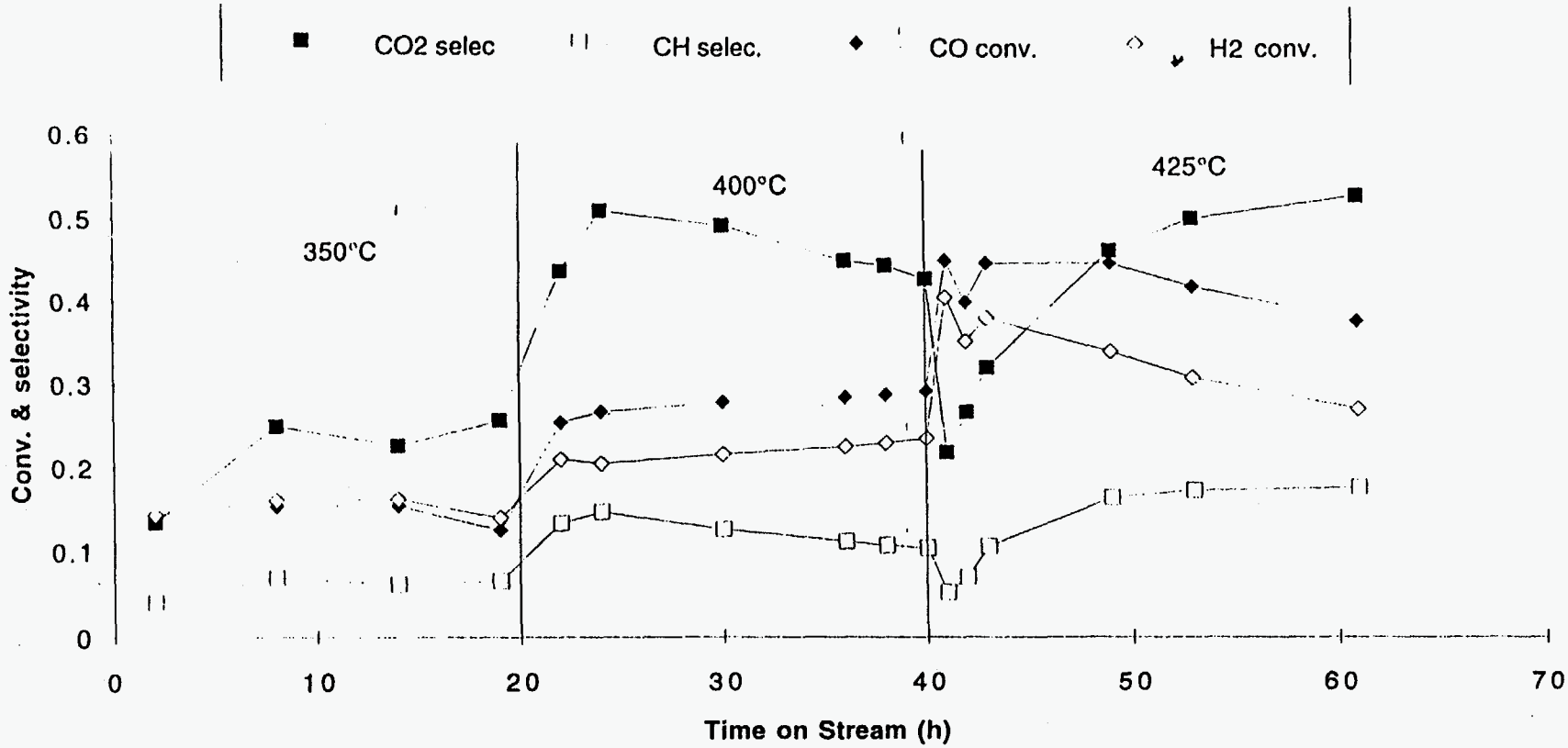

Figure 3.3.3.10. Reaction Performance of F6KOHNCs (350-425°C, 1000 psi, $CO/H_2 = 1$)

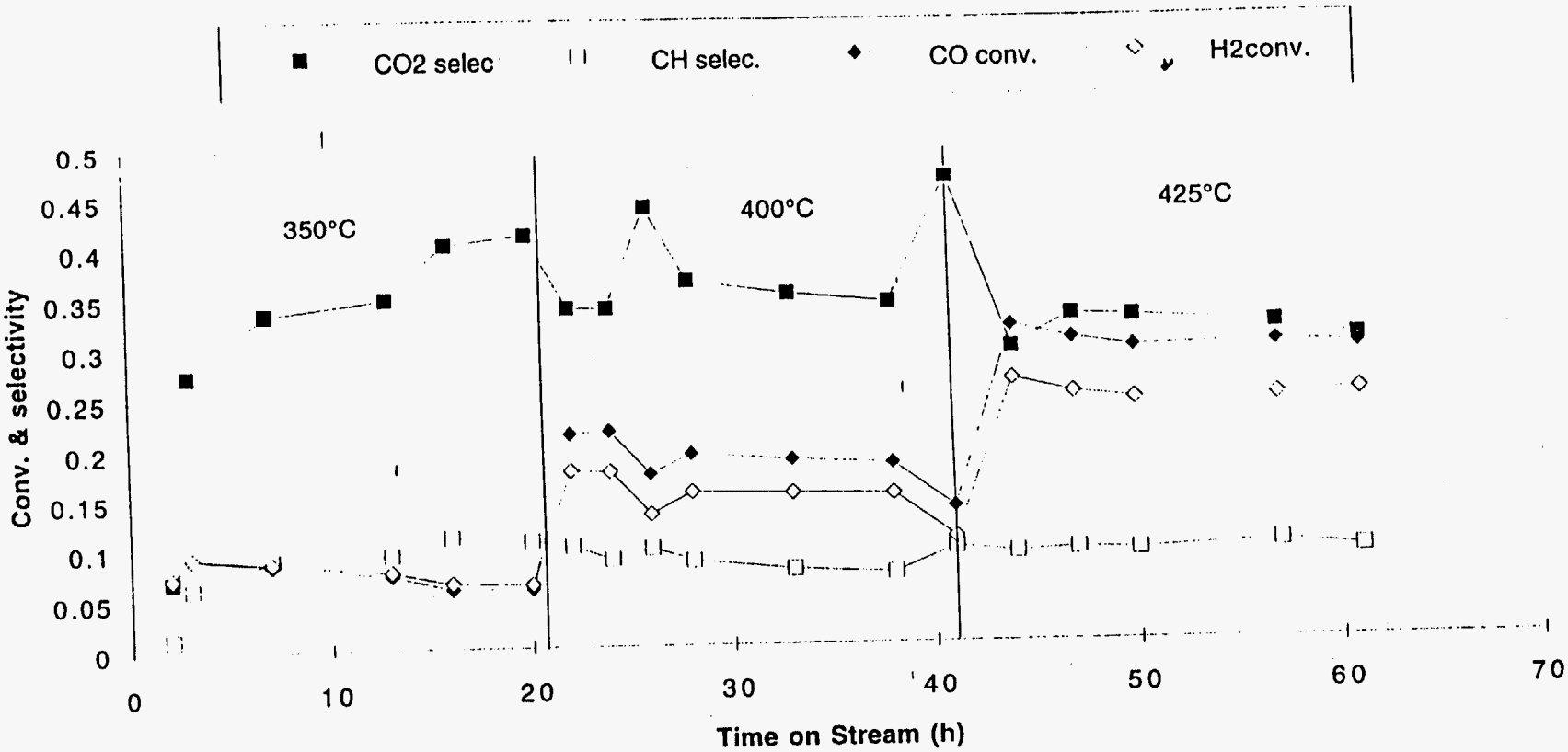

Conclusions

Our findings indicate that calcination is better done under nitrogen, which leads to higher isobutanol selectivity and total alcohol productivity. KOH-precipitated catalysts exhibited enhanced low-temperature performance, high isobutanol selectivity and suppressed n-propanol selectivity at lower temperature. Nitrogen calcination and KOH precipitation do not affect the bulk structure of the catalyst, suggesting that a subtle tuning of the surface sites of the catalysts by these variables may be responsible for the enhanced selectivity. Excess alkali metal doping has been proven to show no beneficial promotional effect on our catalysts.

Future Work

In the next quarterly report, we will present further experimental results on the KOH-precipitated F6KOHN catalyst, examining the effects of reaction pressure, space time velocity, and various transition metal dopings on performance.

TASK 4: PROGRAM SUPPORT

The subcontract with Bechtel to carry out process and economic evaluations in support of the Alternative Fuels and Chemicals program was put in place at the end of March. As noted in the previous quarterly, Bechtel's assignments have expanded beyond the area of syngas generation and cleanup. A combination of reduced manpower at Air Products coupled with Bechtel's abilities in the area of process innovation and techno-economic evaluation is leading to Bechtel's assuming prime responsibility for the work under Task 4.1, Research Support Studies. A FY95 deliverable in this section is the preparation of isobutanol synthesis catalyst performance requirements for coal-based, resid-based and natural gas-based coproduction routes to MBTE. The target in the Alternative Fuels I contract 91990-94) was 50 gms/hr of isobutanol per kg catalyst, this in turn leading ultimately to a MTBE price of $1.20/gal. With a revised target of MTBE @$.70/gal for 1995-2000, the new performance requirements need calculating as guidance for the university programs at Aachen, Delaware, and Lehigh.

TASK 5: PROGRAM MANAGEMENT

5.1 Reports and Presentations

B. L. Bhatt participated in a peer review of proposals to DOE's Advanced Coal Research Program for U. S. Colleges and Universities. A review meeting was held in Pittsburgh on January 30.

Detailed data analysis was performed on the results of the Fischer-Tropsch II run recently completed. A report has been written and is being reviewed internally.

An abstract for a paper entitled "Productivity Improvements for Fischer-Tropsch Synthesis" has been accepted for an oral presentation at the 14th North American Catalysis Society Meeting. The paper, which is co-authored by APCI, DOE and Shell personnel, will be presented by B. L. Bhatt at the Hydrocarbons session on June 15.

5.2 Management Activities

The subcontract with Bechtel was in place by the end of the quarter. Their first priority will be to set performance targets for isobutanol synthesis to meet expected future MTBE values.

We continue to strive towards a subcontract with Eastman Chemical. This will be in place, hopefully, within the next quarter.